11590 Långtidsexponering av betong i marin miljö - utvärdering

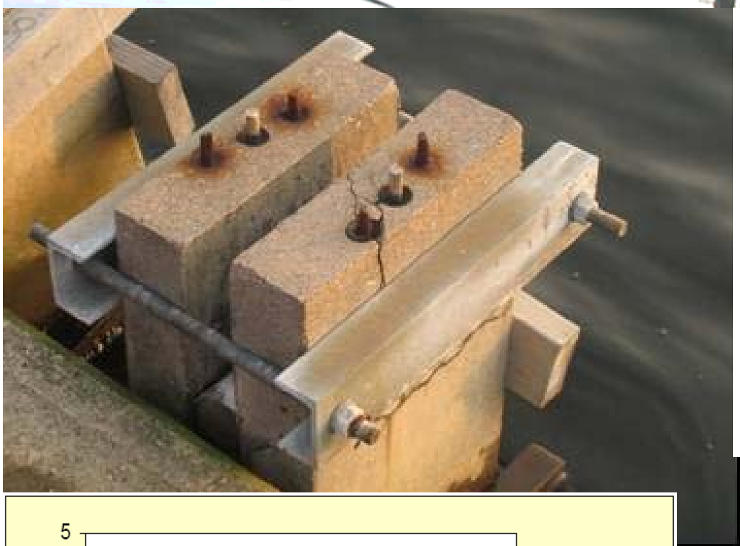

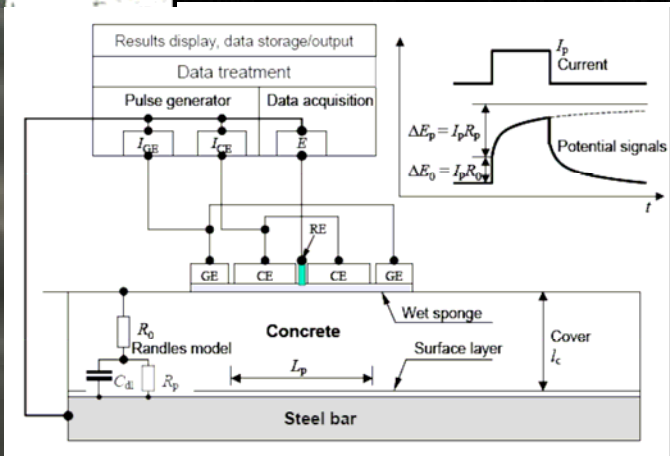

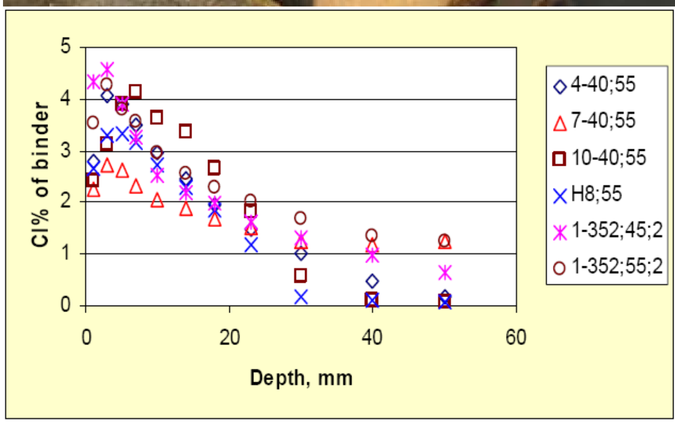

Tang Luping
Peter Utgenannt
Per Fidjestøl

Evaluation of Chloride-Induced Corrosion of Steel in Concrete after Long-Time Exposure in a Marine Environment

SP Report 2005:54
Building technology and Mechanics
Borås 2005

Abstract

Evaluation of chloride-induced corrosion of steel in concrete after long-time exposure in a marine environment

This report presents the results from a SBUF project dealing with the chloride-induced corrosion of steel in concrete. A newly developed rapid non-destructive technique for corrosion measurement was used to assess the conditions of steel embedded in concrete slabs with different types of binder and water-binder ratios. These concrete slabs were exposed in the real marine environments at Swedish west coast (Träslöveläge) and Norwegian south coast (Kristiansand) for 10 to 13 years. Based on the results from the non-destructive measurement, the actual corrosion of steel bars in 9 concrete slabs was visually examined and the chloride profiles in the penetrating direction as well as at the cover level were measured. The results from the visual examination show that the newly developed rapid technique is a useful tool with reasonably good accuracy for assessment of corrosion of steel in concrete. It has been found that the corrosion rate measurement is the most reliable parameter, while the half-cell potential and resistivity can only be used as complementary parameters in the assessment of corrosion status. For the uncracked concrete, the visible corrosions normally occurred about 10-20 cm under the seawater level, where the oxygen may be sufficiently available for initiating the corrosion. As expected, for the cracked concrete, the visible corrosions occurred at the cracks. It is also found that chloride may easily penetrate through a poor interface between concrete and mortar spacer and initiate an early corrosion. As a conclusion, although the chloride level 1% by mass of binder may not be the same as the conventionally defined threshold value, it can be taken as the critical level for significant on-going corrosion that is visible by destructive visual examination, despite of types of binder.

Key words: Chlorides, concrete, corrosion, durability, field exposure, marine environment.

SP Sveriges Provnings- och Forskningsinstitut
SP Rapport 2005:54
ISBN 91-85533-00-9
ISSN 0284-5172
Borås

SP Swedish National Testing and Research Institute
SP Report 2005:54

Postal address:
Box 857,
SE-501 15 BORÅS, Sweden
Telephone: +46 33 16 50 00
Telex: 36252 Testing S
Telefax: +46 33 13 55 02
E-mail: info@sp.se

Content

Preface

Durability of concrete structures concerns the society and has been a focused subject for research during the last decades. Understanding the mechanisms behind deterioration would be the key issue that enables prediction of future degradation rate and decision of necessary actions. This project funded by SBUF, Elkem Materials and Skanska has been a very important milestone in understanding mechanisms because the concrete samples have been exposed to a normal environment during more than 10 years without any acceleration. All tests have also been carried out using the best available technology. The results presented are unique and would be very valuable world vide for researchers and analyses for standardization.
I am proud of the excellence of Swedish researchers in this subject and I could certify that Sweden is still in the frontline within material science.

Kyösti Tuutti
Research Director, Skanska AB

December 2005

Sammanfattning (Summary in Swedish)

I denna rapport presenteras resultat från ett SBUF-finansierat projekt om kloridinducerad armeringskorrosion i betong. En nyligen utvecklad snabb, icke förstörande mätmetod för att utvärdera pågående armeringskorrosion i fält användes. Mätningar gjordes på ett stort antal armerade provkroppar av betong med olika bindemedel, bindemedelshalt och täckskikt. Innan mätning hade provkropparna exponerats mellan 10 och 13 år vid två olika fältprovplatser, en på den svenska västkusten (Träslövsläge) och en på norska sydkusten (Kristiansand). Provkropparna var placerade så att halva provkroppen var i vatten och halva ovan vattenytan. Baserat på resultaten från de icke förstörande mätningarna bestämdes den verkliga korrosionsomfattningen visuellt på 9 olika provkroppar. Dessutom bestämdes kloridprofiler i penetrationsriktningen på ett flertal nivå, såväl under som ovan vattenytan.

Det framgår från resultaten att den nyligen utvecklade mätmetoden snabbt ger värdefull och tillförlitlig information om pågående armeringskorrosion. Resultaten visar att mätning av korrosionshastighet är den mest tillförlitliga metoden medan mätning av ”half-cell” potential och resistivitetsmätning endast bör användas som komplementära mätmetoder.

För osprucken betong startade korrosionen normalt på en nivå 10-20 cm under vattenytan där tillgången på syre är tillräcklig för att korrosion skall initieras. För sprucken betong uppstod, som förväntat, korrosion i sprickorna. Vidare upptäcktes att klorider lätt kan penetrera in i betong genom en ”dålig” kontaktzon mellan betong och distanskloss av bruk, vilket leder till en snabb initiering av korrosion.

Resultaten från projektet indikerar att 1% kloridhalt (bindemedelsvikt) kan anses vara ett kritiskt värde för pågående armeringskorrosion detekterbar vid visuell examination. Detta gäller oberoende av bindemedelstyp.

1 Introduction

About 25 years ago, Tuutti [1] made a comprehensive study of corrosion of steel in concrete and presented a conceptual model for service life prediction of reinforced concrete structures. In the beginning of 1990s', a Nordic research project BMB – "Durability of Concrete in Marine Environment" was initiated and followed by several other projects. The work of the BMB project was divided into three research areas: Durability with regard to frost attack, Durability with regard to corrosion of steel, and Transport mechanisms with regard to ingress of moisture and chlorides. Research on frost attack was primarily carried out at SP and research on corrosion was primarily carried out at Cementa and CBI (Cement and concrete institute). Research on transport mechanisms was primarily carried out at Chalmers University of Technology. Further information about the BMB-project and some early results from the projects can be found in [2].

Within the research area "Durability with regard to corrosion of steel", some studies of corrosion mechanisms were carried out by Sandberg at Cementa and resulted in his doctoral thesis entitled "Chloride initiated reinforcement corrosion in marine concrete" [3]. Some laboratory investigations on threshold chloride values were carried out by Pettersson at CBI and the results were reported in [4,5].

Within the research area "Transport mechanisms" a large number of specimens of different concrete compositions have regularly been investigated (2, 5 and 10 years of exposure). The results from these measurements have been presented in a number of Lic/Dr theses from the division of Building Material at Chalmers University of Technology. One example is the thesis by Tang entitled "Chloride Transport in Concrete – Measurement and Prediction" [6]. In this thesis the results from the exposure site were used for developing and calibrating a new test method for evaluating chloride ingress in a marine environment. The test method has been further developed and was adopt as a Nordic standard method NT Build 492, which has been used in many countries worldwide. Results from research carried out at Träslövsläge have also been used in a number of Nordic and European research projects, such as the Nordic project Hetek – "High quality concrete, the Contractors' TEChnoloty"(1996-1997), the European project DuraCrete – "Probabilistic performance based durability design of concrete structures" (1995-1999) and the European project ChlorTest "Resistance of concrete to chloride ingress – from laboratory tests to infield performance" (2003-2005).

Also in Norway much research in corrosion behaviour of steel in the chloride environment has been carried out, with a number of field trials established. In connection with the Swedish project "High Performance Concrete", field exposure was performed in Kristiansand, and results from this project have been published elsewhere [7]. Some guidelines based on the experiences from this and other projects are given in Chapter 14 of Swedish Handbook of Concrete [8].

Although research on durability of concrete has been carried out for a long time, in Scandinavia as well as internationally, there is still a lack of knowledge, especially with regard to the threshold chloride values for initiating corrosion. An increased knowledge would lead to more cost effective buildings and more reliable service life predictions. As an example there is a need for better, more reliable models for the initiation and propagation of reinforcement corrosion. Existing models are rough and there is a lack of consensus within the research community about the validity of the models. To develop more precise models and calibrate them against reality data from field investigations on constructions exposed to well-defined environments over a long time is needed. The SBUF project presented in this report is primarily to investigate the conditions of steel in the concrete slabs exposed at the field test sites and measure the chloride contents at the positions where depassivation of steel has been detected. From the relationships between corrosion condition and chloride content it is possible to evaluate the threshold chloride level for initiation of corrosion of steel in concrete exposure in the real marine environment. The results presented in this report can be used for improving or developing better models and for calibration against reality.

2 Field Exposure Sites

2.1 Träslövsläge exposure site (Sweden)

The field exposure site in Träslövsläge harbour was established in 1991 and was initially used as field test site within the Nordic research project BMB – Durability for concrete in marine environment. In this project a number of companies (Cementa, Finnsementti, Norcem, Skanska), Universities (Chalmers, Lund Institute of Technology), technical institutes (Swedish National Testing and Research Institute, Swedish Cement and Concrete Institute, VTT) as well as authorities (Swedish National Road Administration) and research funds (BFR, FORMAS, SBUF) took part.

The primary reason for starting a project about durability of concrete in marine environment was the need for evaluating and calibrating laboratory test methods against reality. Another reason was the plans for building a connection (bridge and tunnel) between Denmark and Sweden. The building industry realised the need for more knowledge and experience of durability in the field to build a connection with a long service life.

The field exposure site is situated in Träslövsläge harbour in the south western part of Sweden, 80 km south of Gothenburg. Three pontoons are placed behind a pier in the harbour (figure 1). Since 1991 a large number of specimens from different projects have been placed on top and on the sides of the concrete pontoons. The specimens investigated in this project were cast during the winter 1991/1992, and were placed at the earliest one week and at the latest one month after casting. In total there are around 40 concrete qualities (different binders, w/b-ratio and air contents) at the test site. Information about the concrete qualities can be found in [2]. The test specimens are slabs (height 100 cm, width 70 cm, thickness 10-20 cm). The panels are reinforced with rebar with different covers, between 10 – 30 mm.

Figure 1 – Swedish field site at the Träslövsläge Harbour, Varberg.

2.2 Kristiansand exposure site (Norway)

The field exposure site in Kristiansand was established in 1994 as part of the Swedish project High Performance Concrete. The primary purpose of the facility was to study the effect of cracks on samples partly submerged in sea water. (A lab study accompanied the field testing)

The exposure facility, a concrete pontoon with samples attached along the sides, was located at the end of the main wharf of Elkem’s Fiskaa smelting plant, in an exposed marine situation (figure 2). After a few years, the pontoon was moved a little to the east, and remained here for a few more years. Because of the wear and tear, the pontoon was eventually moved to the north end of the main wharf, where it remains today. It can be mentioned that the Norwegian Road Directorate has established their own pontoon for testing of concrete compositions versus chloride ingress, a test that has now been running for 10 years.

Figure 2 – Norwegian field site at the main wharf of Elkem’s Fiskaa smelting plant, Kristiansand.

3 Measurement Methodology

3.1 Technique for corrosion measurement

In this project, a handheld instrument RapiCor, which is based on the rapid technique newly developed at SP [9, 10], was used for measurement of corrosion of steel in concrete, see figure 3. The instrument measures half-cell corrosion potential, and then generates two gulvanostatic pulses for corrosion rate and resistivity measurements. The measurement is quick and only needs a few seconds to obtain three parameters: corrosion potential, corrosion rate of steel and resistivity of concrete. These three parameters contribute a more accuracy estimation of the corrosion status of steel.

Figure 3 – Newly developed handheld instrument.

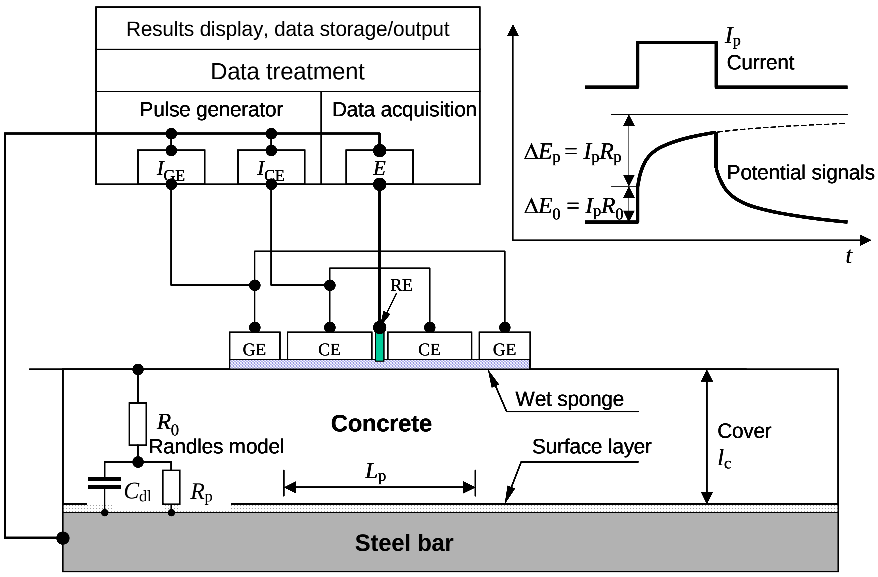

Figure 4 – Measurement principle of the new instrument.

The measurement principle of the new rapid technique is illustrated in figure 4. In order to facilitate the modelling of electrical current distributions using 2-D numerical model, the rectangular shape of counter and guard electrodes were used in this new technique. A wet sponge is place on concrete surface in order to improve the contact between concrete and the electrodes unit. Similar to the typical galvanostatic pulse measurement, the instrument firstly measures the corrosion potential E_{corr} by the reference electrode placed at the centre of the electrodes unit and afterwards imposes galvanostatic currents I_{CE} and I_{GE} through the counter electrodes "CE" and the guard electrodes "GE" to the steel bar embedded in concrete. Immediately after having imposed the currents I_{CE} and I_{GE}, the data acquisition system starts to record the signal responses of potential $\Delta E_a(t)$ at a time interval of less than 0.02 seconds. The recorded potential-time curve is directly displayed on the screen of the instrument and can be used for calculation of various parameters such as ohmic resistance R_{Ω}, polarization resistance R_p, etc.

For an "endless" long steel bar embedded in concrete, the imposed total current $I_{tot} = I_{CE} + I_{GE}$ will disperse along the steel bar to a certain distance, depending on the conductivity of concrete, σ_c, the thickness of concrete cover, l_c, and the conductivity of the surface film of the steel, σ_f. Therefore, it does not necessarily mean that the current I_{CE} is equal to the polarization current I_p through the specified polarization length L_p. In order to calculate the proper polarization current I_p through the specified polarization length L_p the numerical modelling must be used. In this new technique, a 2-D FEM (2-Dimensional Finite Element Method) was employed to model the current distributions under the galvanostatic measurement conditions. With the help of modelling the effective polarization current I_p flowing through the specified polarization length L_p can be estimated from the ratio of polarization potential to Ohmic drop, both of which can be obtained from the measurement. Therefore, the true Ohmic and polarization resistances, R_{Ω} and R_p, can be calculated using Ohm's law and, consequently, the resistivity of concrete and the corrosion rate can be obtained.

Through a Nordtest project the new technique together with other techniques were compared with the destructive gravimetric method [11]. The results from a comparative measurement on both small and large reinforced concrete slabs show that the corrosion rate measured by the new rapid technique is quite comparable with that measured by the Gecor instrument, which uses modulated confinement technique. Similar to the Gecor instrument, when the measured value is multiplied by a pitting factor of 6 for the slabs containing certain amount of chloride, the measured corrosion rate becomes fairly comparable with the actual one by the gravimetric method.

3.2 Concrete slabs at the Träslövsläge field site

3.2.1 Primary field investigation

There were more than 40 concrete slabs from the previous BMB project [2] continuously exposed at the field site. The mixture proportions of concrete are summarised in Table 1. As the first step to make a rough estimation of the corrosion status, the corrosion measurement was carried out with the slabs kept in place, that is, a half of the slab was exposed under the seawater and another half to the air. The position above the seawater level was chosen for the measurement, as shown in figure 5, left side. The results are listed in Appendix 1.

Table 1 – Mixture proportions of concrete exposed at the Träslövsläge field site.

Mix No.	Binder type	Binder kg/m³	Water-binder ratio[1)]	Fine aggreg. 0-8 mm kg/m³	Coarse aggreg. 8-16 mm kg/m³	Sp[2)] % of binder	AEA[3)] % of binder	Air content %	28d compr. Strength[4)] MPa
1-35	100%Anl[5)]	450	0.35	839	839	1	0.041	6.0	70
1-40	100%Anl[5)]	420	0.40	873	806	0.8	0.03	6.2	58
2-35	100%Slite[6)]	450	0.35	801	868	1.7	0.038	5.7	60
2-40	100%Slite[6)]	420	0.40	871	804	1.3	0.029	6.2	54
2-50	100%Slite[6)]	390	0.50	853	787	-	0.026	5.8	42
3-35	95%Anl+5%SF[7)]	450	0.35	801	868	1.2	0.08	5.8	72
3-40	95%Anl+5%SF[7)]	420	0.40	835	835	0.8	0.043	6.1	61
4-40	90%Anl+10%SF	420	0.40	803	870	1.17	0.043	6.6	65
5-40	95%Anl+5%SF	420	0.40	878	878	1.5	0.006	2.9	81
6-35	95%Anl+5%SF	450	0.35	858	929	1.5	-	2.1	93
6-40	95%Anl+5%SF	420	0.40	898	898	1.5	-	1.7	87
7-35	100%Anl	450	0.35	898	898	1.5	-	2.4	91
7-40	100%Anl	420	0.40	939	867	1	-	2.1	79
8-35	100%Slite	470	0.35	847	918	1.8	-	2.1	73
8-40	100%Slite	440	0.40	882	882	1.5	-	2.1	67
8-50	100%Slite	410	0.50	893	924	-	-	1.4	56
10-40	78.5%DK+17%FA[9)]+ 4.5%SF	420	0.40	770	905	1.7	0.063	6.1	69
11-35	85%DK+10%FA+5%SF	450	0.35	781	917	2.33	0.04	5.7	84
12-35	85%Anl+10%FA+5%SF	450	0.35	781	917	1.87	0.055	6.4	73
H1	95%Anl+5%SF	500	0.30	836	942	2.3	-	0.8	112
H2	90%Anl+10%SF	500	0.30	820	963	2.1	-	1.1	117
H3	100%Anl	492	0.30	791	892	2.7	-	3.6	96
H5	95%Anl+5%SF	551	0.25	806	946	3	-	1.3	125
H6	95%Anl+5%FA	518	0.30	791	892	2.5	-	2.8	95
H7	95%Deg400[10)]+5%SF	500	0.30	836	942	2.3	-	1.3	117
H8	80%Anl+20%FA	616	0.30	680	865	2.8	-	3.0	98
H9	100%Deg400	500	0.30	812	916	2.3	-	2.9	102

1) Assuming that the efficiency factor of silica fume is 1 and fly ash is 0.3.
2) Sp – Super-plasticizer. Cementa 92M
3) AEA – Air entraining agent. Cementa L14
4) According to SS 13 72 10
5) Anl - Anläggningscement (Swedish SRPC)
6) Slite - Slite cement (Swedish OPC)
7) SF - Silica fume (Elkem. Norway)
8) DK - Aalborg Lav cement (Danish SRPC)
9) FA - Fly ash (Aalborg . Denmark)
10) Deg400 - Degerhamn 400 cement (another type of Swedish SRPC)

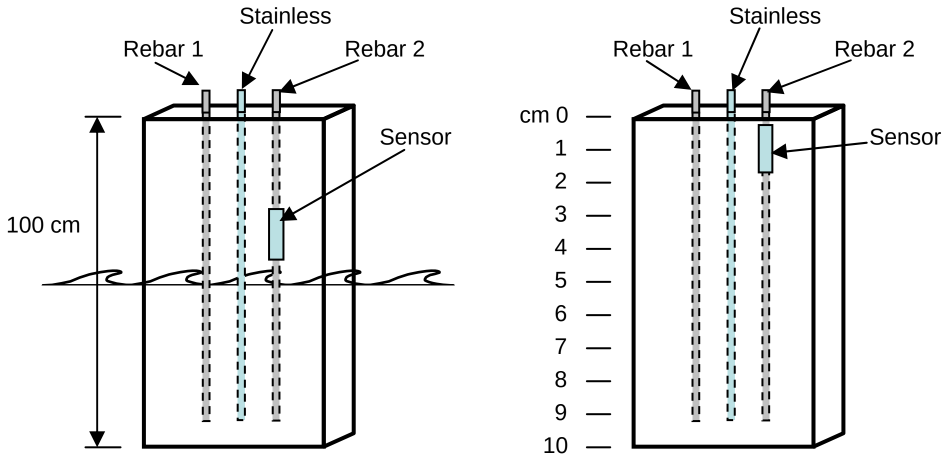

Figure 5 – Measurement positions, left: in place, right: in the laboratory or lifted up.

According to this rough estimation, taking into account both the roughly measured corrosion risk index and the type of concrete, it was decided to take five slabs (see Table 2) to the laboratory for further investigation.

Table 2 – Concrete slabs taken from Träslövsläge for the laboratory investigation.

Mix No.	Binder type	Binder kg/m^3	Water-binder ratio	Air content %	28d compr. strength MPa	Rebar diam. mm	Cover mm Bar 1/2	Cl % of binder 2) at cover depth Bar 1/2	Corrosion risk index 3) Bar 1/2
1-352 1)	100%Anl	450	0.35	6.0	70	20	20/15	2/2.4	4/4
4-40	90%Anl+10%SF	420	0.40	6.6	65	12	15/15	1.6/1.6	4/2
7-40	100%Anl	420	0.40	2.1	79	12	10/15	2.6/2.1	3/2
10-40	78.5%DK+17%FA+ 4.5%SF	420	0.40	6.1	69	12	15/10	2.5/3.3	3/4
H8	80%Anl+20%FA	616	0.30	3.0	98	12	15/10	1.7/2.3	4/3

1) The last number "2" denotes the second batch in concrete casting.
2) Data quoted/interpolated from the investigation after 10 years' exposure [12].
3) According to the preliminary field investigation, see Appendix 1.

3.2.2 Corrosion measurement in the laboratory

These five slabs were taken from the field site and covered with thick plastic sheet, and transported to SP's laboratory, where the corrosion measurements were carried out twice with an interval of five days, at the positions with an interval of 10 cm from the top edge of the slab, as shown in figure 5, right side. The measurement results are listed in Appendix 2. After the second measurement, a groove along each rebar was cut from the backside of the slab, so as to facilitate the release of rebar for visual examination in order to verify the non-destructive measurement, see figure 6.

Figure 6 – Release of steel bars for visual examination.

3.2.3 Measurement of chloride content

After release of rebar, concrete samples were taken at the depth where the rebar was embedded and at the positions where the corrosion was measured by the RapiCor technique, see figure 7. From each slab, cores were taken at the vertical distance 45 and 55 cm from the top edge (representing splash zone) and the horizontal distance about 50 mm away from the side edge (avoiding two-dimensional penetration) for determination of chloride penetration profiles. The concrete profiling and analysis of acid soluble chloride and calcium content in each sample were carried out at Chalmers, using the same techniques as used in the previous investigations, e.g. in [12].

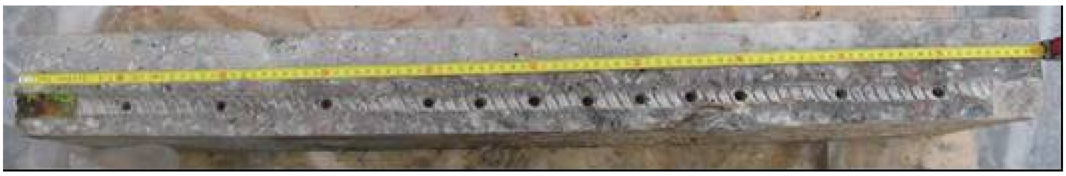

Figure 7 – Sampling for chloride analysis.

3.2.4 Further corrosion measurement in the field

Based on the visual examination of the steel bars from the five selected slabs, it has been verified that the non-destructive RapiCor technique gives satisfactory estimation of corrosion, as will be presented in the next chapter. Therefore, it was decided to use this technique for the rest of slabs exposed in the Träslövsläge field site. In this case, the slabs were lifted up and the measurement was carried out at the positions as shown in figure 5, right side. The measurement results are listed in Appendix 3. The values of maximum corrosion rate on each steel bar are summarised in figures 8 and 9. It seems not clear to find the effect of water-binder ratio and type of binder on corrosion rate, due to the fact that the poor interface between concrete and distance spacer resulted in early corrosion. On the other hand, the corrosion rate was found relatively low when cover thickness is larger than 30 mm. Therefore, as general conclusions, thicker cover is an effective way to protect the steel from corrosion.

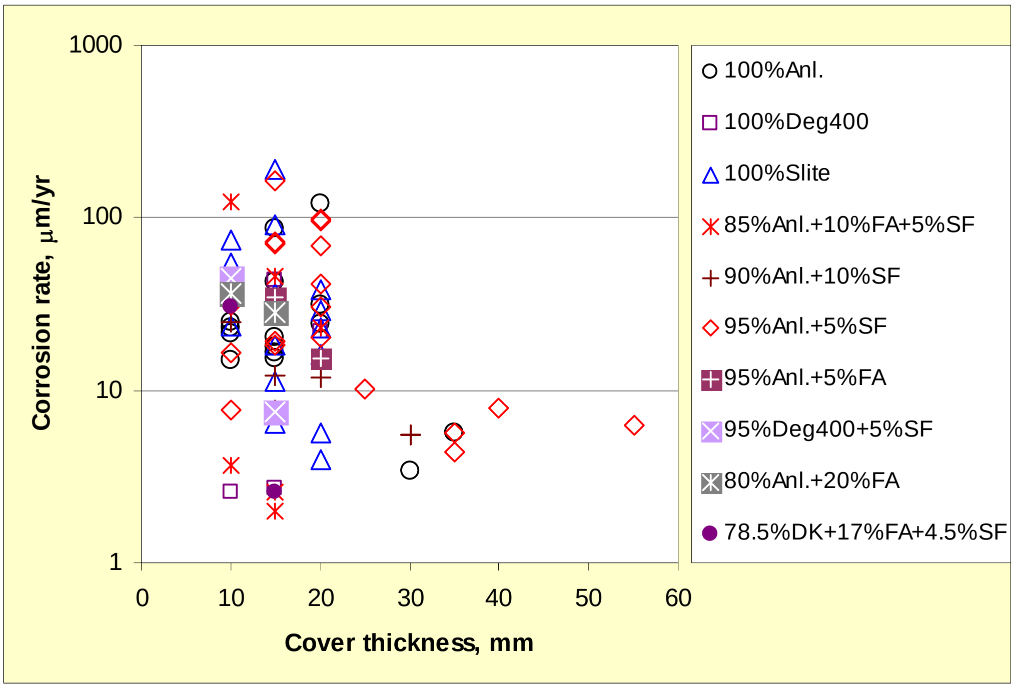

Figure 8 – Summary of corrosion rate in concrete with different types of binder.

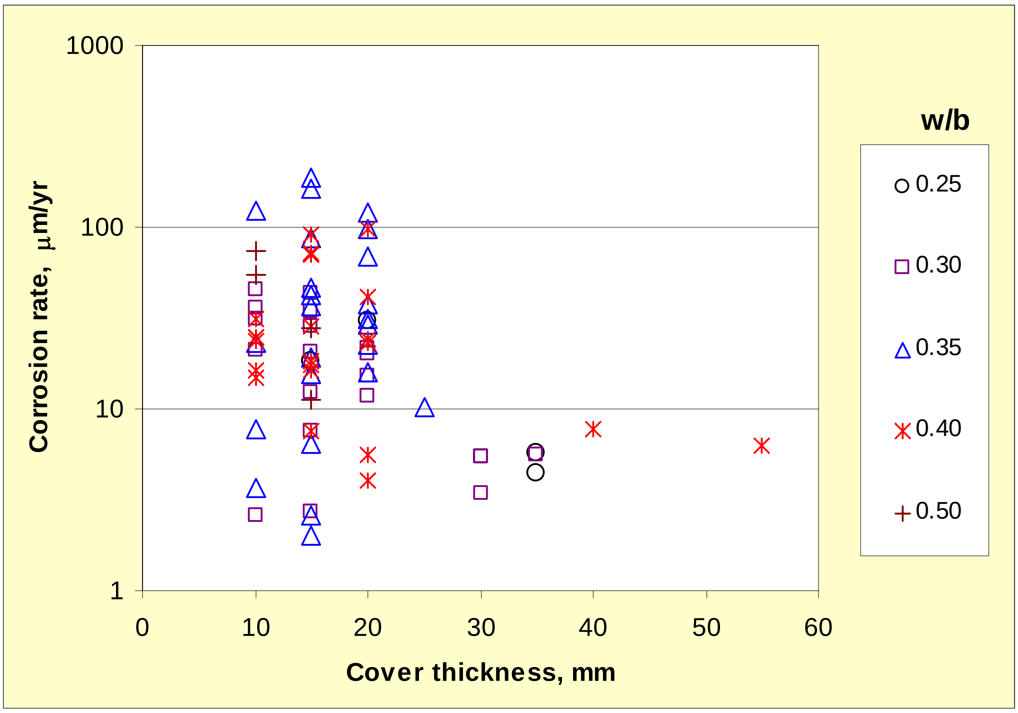

Figure 9 – Summary of corrosion rate in concrete with different water-binder ratios.

3.3 Concrete slabs at the Kristiansand field site

3.3.1 Corrosion measurement in the field

There were totally 25 slabs of size 1000×400×100 mm exposed at the Kristiansand field site, but two of them (Slabs 2a and 2b) were dropped in the deep water. The mixture proportions of concrete are summarised in Table 3. Figure 10 shows the positions of the concrete slabs around the pontoon. The slabs were intentionally cracked by tightening two slabs back-to-back with bolts in such a way as shown in figure 11. Similar to the measurement carried out at the Träslövsläge field site, the slabs were lifted up and the measurement was carried out at the similar positions as shown in figure 5, right side. The results are listed in Appendix 4

Table 3 – Mixture proportions of concrete exposed at the Träslövsläge field site.

Mix No.	Binder type	Cement kg/m³	Water-binder ratio	Fine aggreg. 0-8 mm kg/m³	Coarse aggreg. 8-16 mm kg/m³	Sp % of binder	Air content %	28d compr. Strength MPa
30A	100%Anl[1)]	491	0.30	862	946	1.77	2.43	92
30S	100%Slite[2)]	490	0.30	881	928	2.1	2.33	83
25A 5S	95%Anl+5%SF[3)]	523	0.25	835	980	3.15	0.85	118
30A 5S	95%Anl+5%SF	475	0.30	864	947	1.4	0.8	103
40A 5S	95%Anl+5%SF	399	0.40	927	906	1.19	0.55	82
30S 5S	95%Slite+5% SF	475	0.30	866	917	2.8	1.1	91.5
30A 10S	90%Anl+10%SF	450	0.30	863	956	2.46	0.85	118
30A 15S	85%Anl+15%SF	450	0.30	806	930	2.38	0.75	112
30A 25FA	75%Anl+25%FA	487	0.30	682	854	1.89	2.15	80
30A 35FA	65%Anl+35%FA	422	0.30	699	838	1.89	1.55	78

1) Anl - Anläggningscement (Swedish SRPC)
2) Slite - Slite cement (Swedish OPC)
3) SF - Silica fume (Elkem. Norway)
4) FA - Fly ash (Aalborg . Denmark)

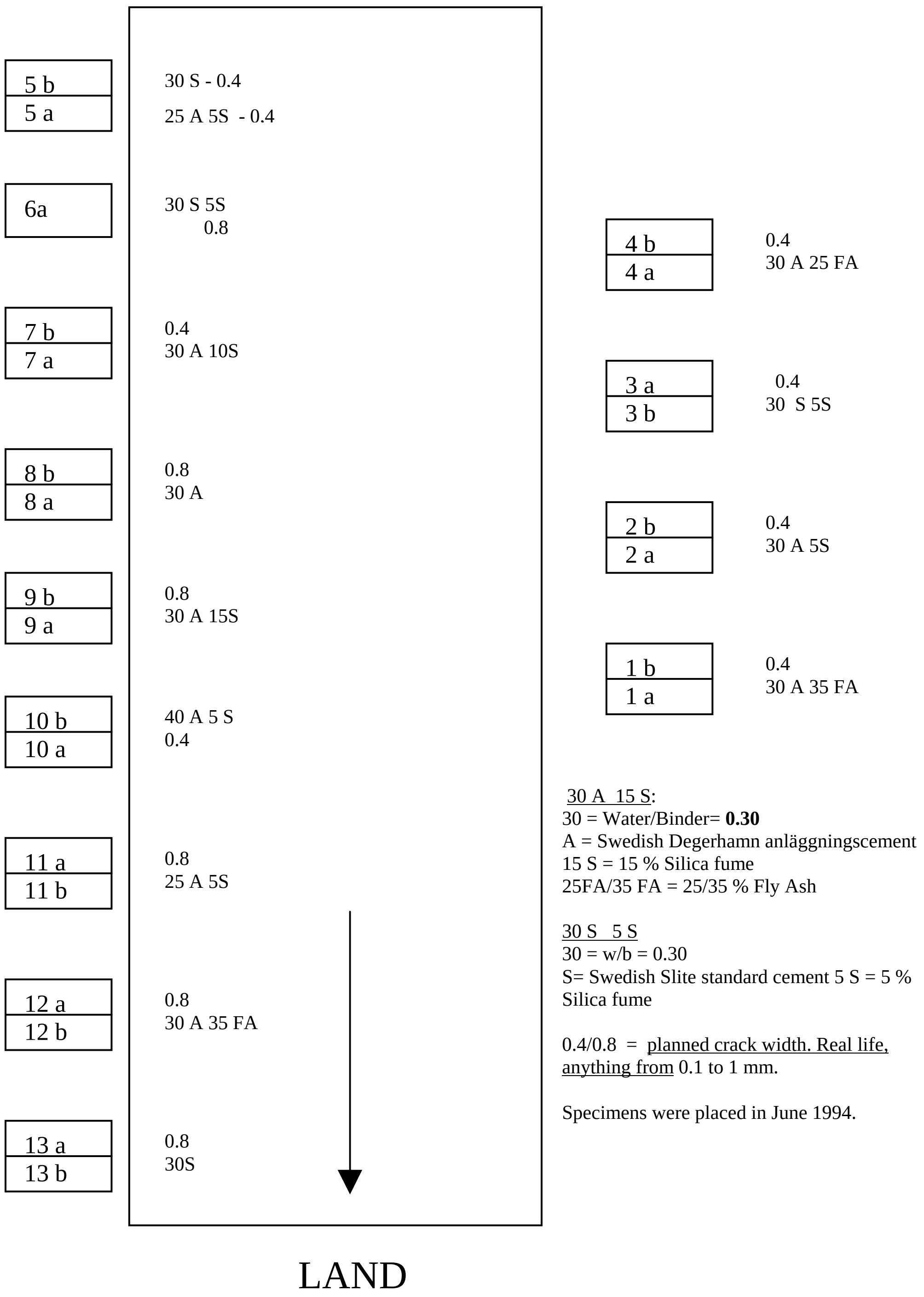

Figure 10 – Schematic of concrete slabs at the Kristiansand field site.

Figure 11 – Intentional cracks in the slabs at the Kristiansand field site.

3.3.2 Visual examination and chloride analysis

After the field measurement, four slabs (1a, 7a, 8a and 10a, all with Swedish Anläggningscement, as shown in Table 4) were transport to SP for further visual examination and chloride analysis in the similar way as described in 3.2.3. Owing to the introduced cracks, it is difficult to take the samples following the same positions as used for the Träslövsläge slabs. Therefore, only six samples were taken from each slab, three from the cover depth 15 mm at the distance about 25, 50 and 75 mm from the top edge and other three from the cover depth 30 mm at the positions where corrosion was detected.

Table 4 – Concrete slabs used for further investigation at the laboratory.

Slab	Mix No.	Intended crack width mm	Silica fume %	Fly Ash %	Water/binder ratio
1a	30A 35FA	0.4	0	35	0.3
7a	30A 10S	0.4	10	0	0.3
8a	30A	0.8	0	0	0.3
10a	40A 5S	0.4	5	0	0.4

4 Results and Discussions

4.1 Verification of the non-destructive measurements

The results from visual examination compared with the non-destructive measurements on totally 9 slabs including 18 rebars are shown in Appendix 5. A typical example is given in figure 12. It can be seen that the half-cell potential is in many measurement points very negative, implying 90% possibility for on-going corrosion according to ASTM C876, even for the stainless bar! The visual examination shows that there is no any mark of corrosion on the stainless bar. The resistivity of concrete measured on each rebar is similar, that is, the upper 20~30 cm part of concrete is relatively dry, while the lower part is wet. Therefore, the parameter resistivity alone cannot be used for the judgement of corrosion. On the other hand, the corrosion rate measurement can clearly allocate the pitting positions, as the maximum value of corrosion rate at the 70 cm on Rebar 2.

From the results it can be concluded that the corrosion rate measurement is the most accurate way to find the active corrosion of steel in concrete when compared with the half-cell potential and resistivity measurements. The results from the Träslövsläge slabs show that the visible corrosions normally occurred about 10~20 cm under the seawater level, where the oxygen may be sufficiently available for initiating the corrosion. Some of the corrosion was found at the lower end of the rebar (see the lower left part in figure 12), probably due to the poor interface between the concrete and the mortar spacer. Once the pitting corrosion occurs, it will cathodically protect the adjacent area of the rebar from corrosion, but will interfere in the measurements at the adjacent positions. It is interesting to point out that, even though the upper end of the rebar is corroding (see the upper left part in figure 12), it will not interfere in the measurement at the adjacent positions, probably due to the relatively dry concrete, which electrically isolates the corrosion area. For the Kristiansand slabs, the visible corrosions normally occurred at the cracks, as shown in figure 13.

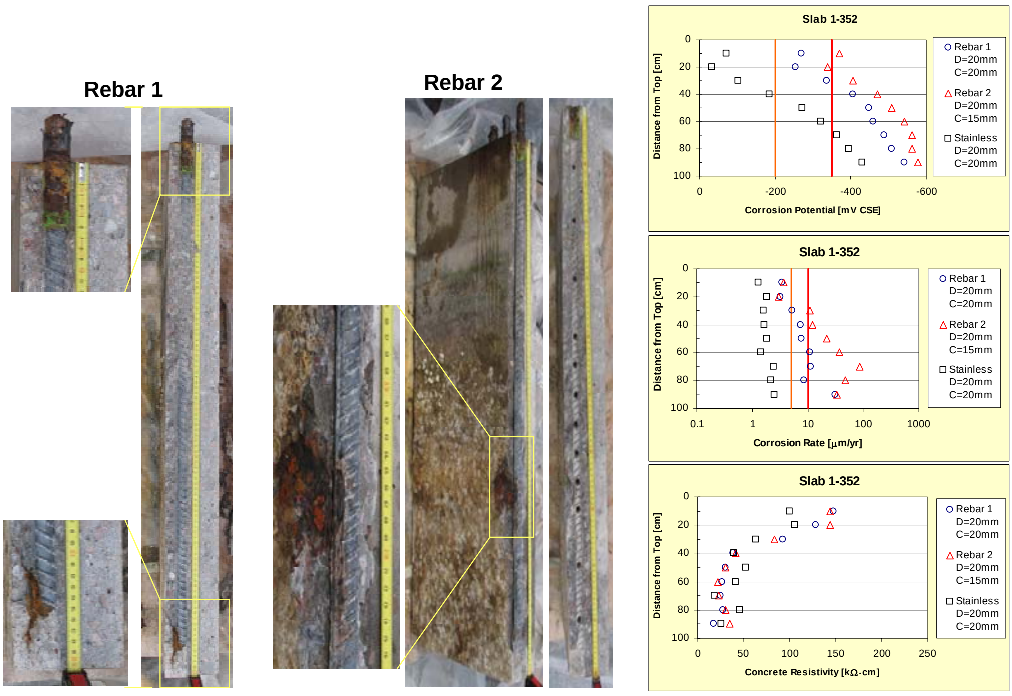

Figure 12 – Example of visual examination results from the Träslövsläge slab.

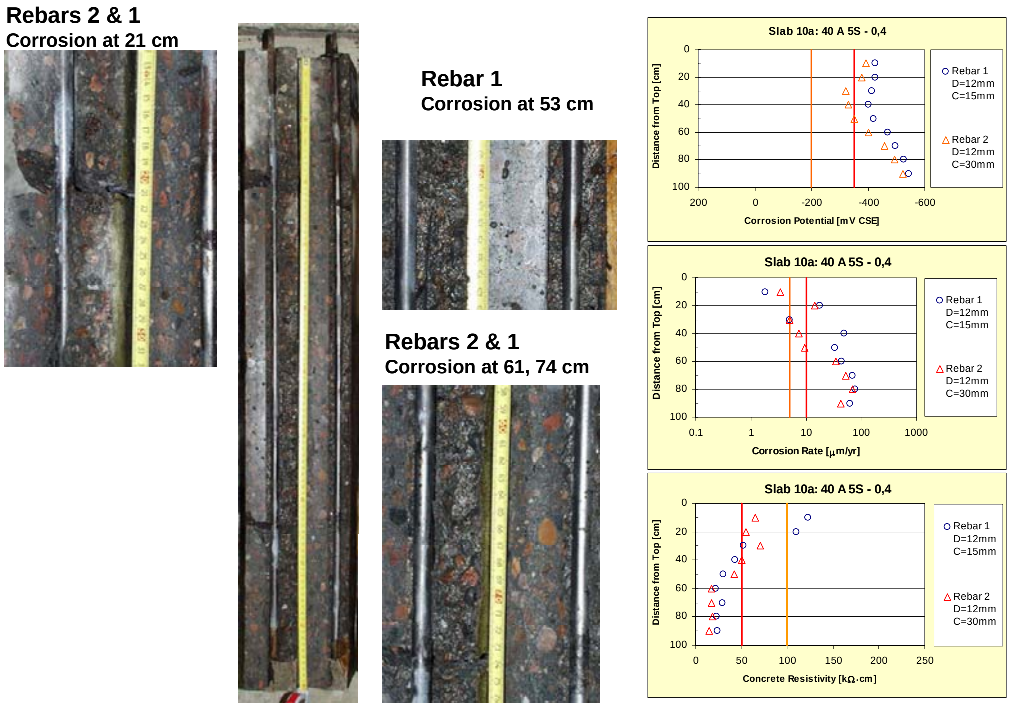

Figure 13 – Example of visual examination results from the Kristiansand slab.

4.2 Chloride content at the cover level

The results of chloride content measured at the cover level measured from the Träslövsläge slabs are summarised in figure 14 and those from the Kristiansand slabs are summarised in figure 15. It can be seen from figure 14 that the chloride content under the water level is normally over 1% by mass of binder, except for one point in the fly ash concrete H8 at cover 15 mm. The chloride content in the Kristiansand slabs is in general higher than in the Träslövsläge slabs. The higher salt concentration in the Kristiansand seawater is one reason while the cracks introduced in the Kristiansand slabs can be another reason for the higher chloride content as shown in figure 15.

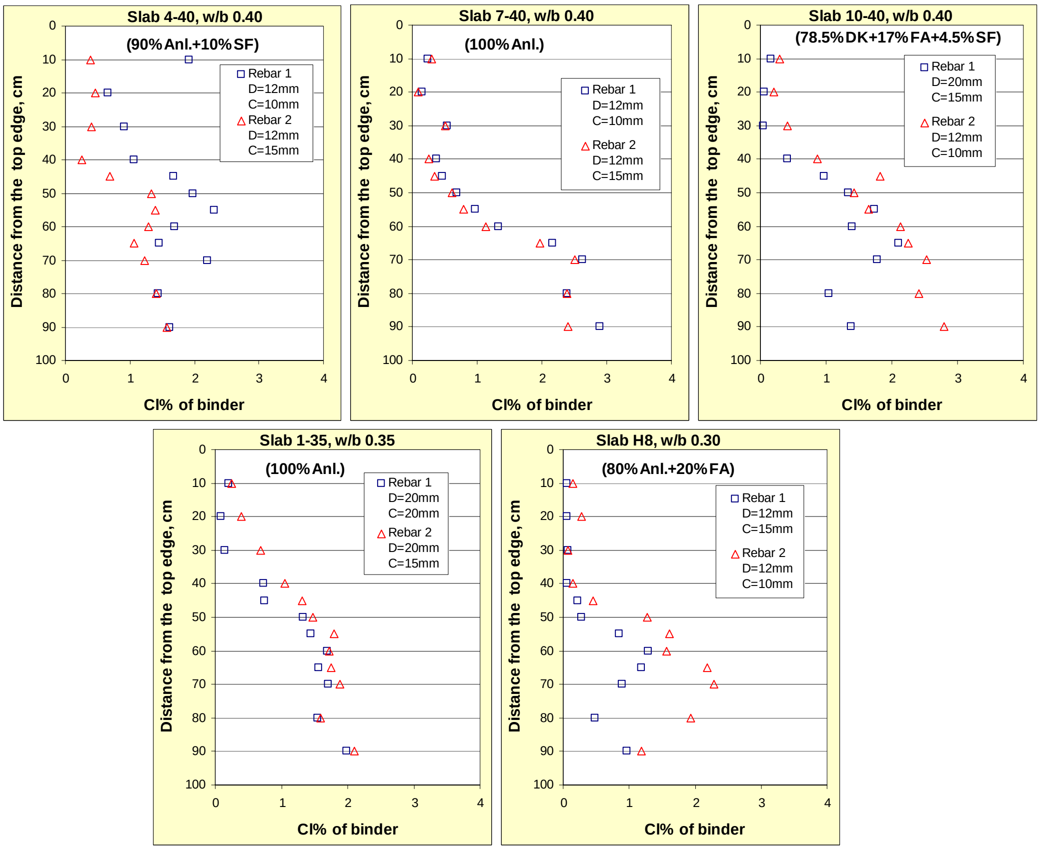

Figure 14 – Results of chloride content measured at the cover level from the Träslövsläge slabs.

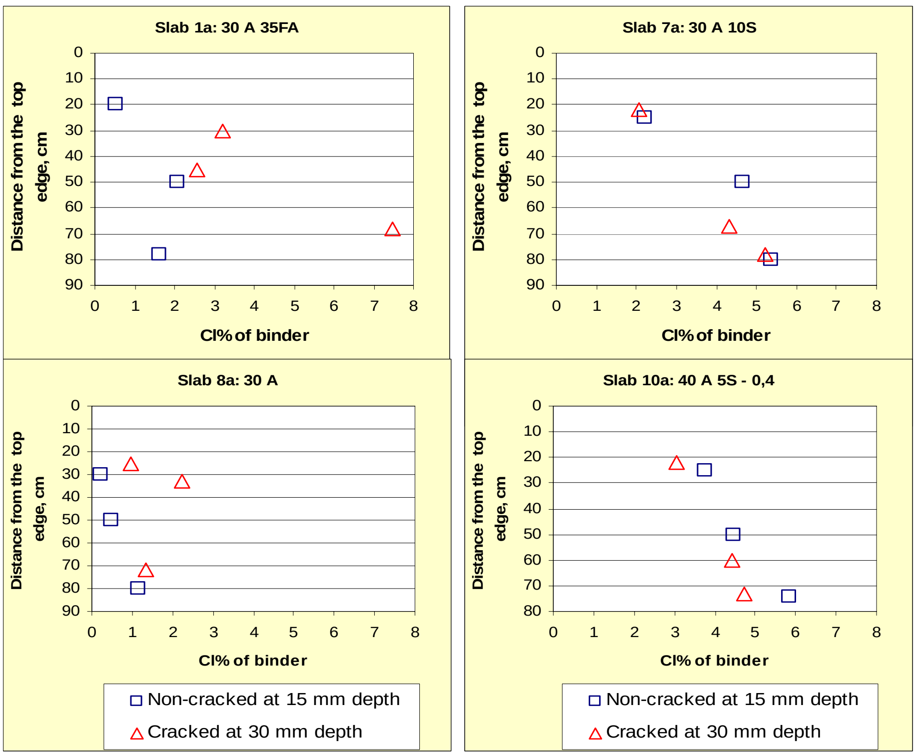

Figure 15 – Results of chloride content measured at the cover level from the Kristiansand slabs.

4.3 Chloride profiles

The results of chloride penetration profiles are summarised in figure 16. It can be seen that the chloride profiles measured from the same slab (1-352) at the positions 45 cm and 55 cm from the upper edge are reasonably in agreement. It is natural that the chloride penetration at position 55 cm is relatively higher that that at position 45 cm. It is interesting to see that, after 13 years' exposure, the chloride penetration level 1% binder has reached at 50 mm depth for Portland cement concrete with w/b 0.35, and over 25 mm depth for all other types of concrete including silica fume and fly ash with w/b 0.30. These results are very comparable with those measured after 10 years' exposure [12], as shown in figure 17. It should be noted that the 10 years' measurements were carried out at SP, while the 13 years' measurements were carried out at Chalmers by different operators, but the similar techniques for grinding and chloride analysis. These comparable results indicate that the measurement techniques for chloride penetration profiles used in Sweden are reasonably reliable.

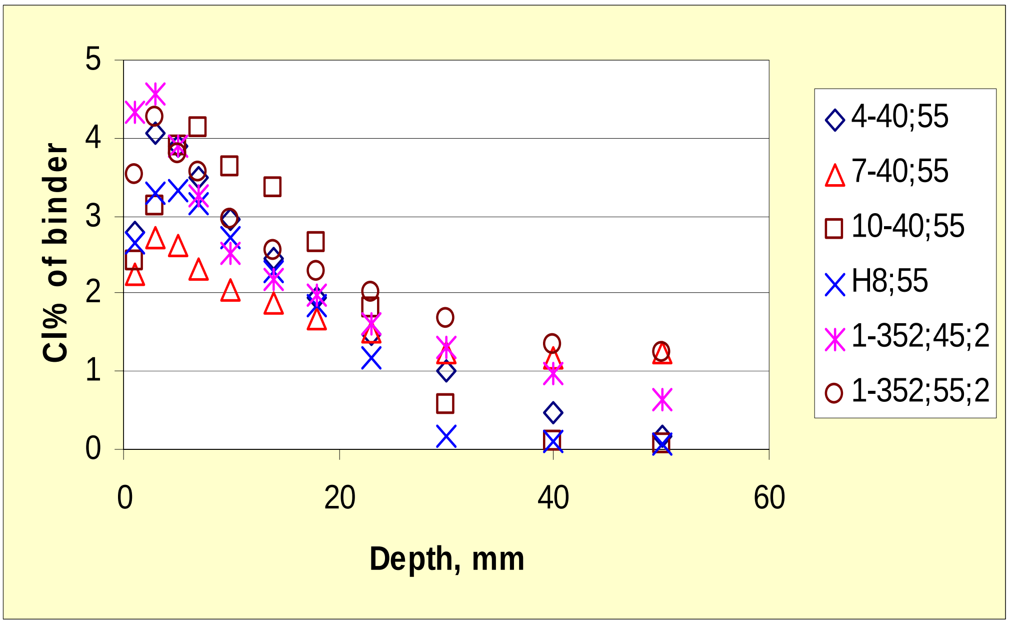

Figure 16 – Results of chloride penetration profiles.

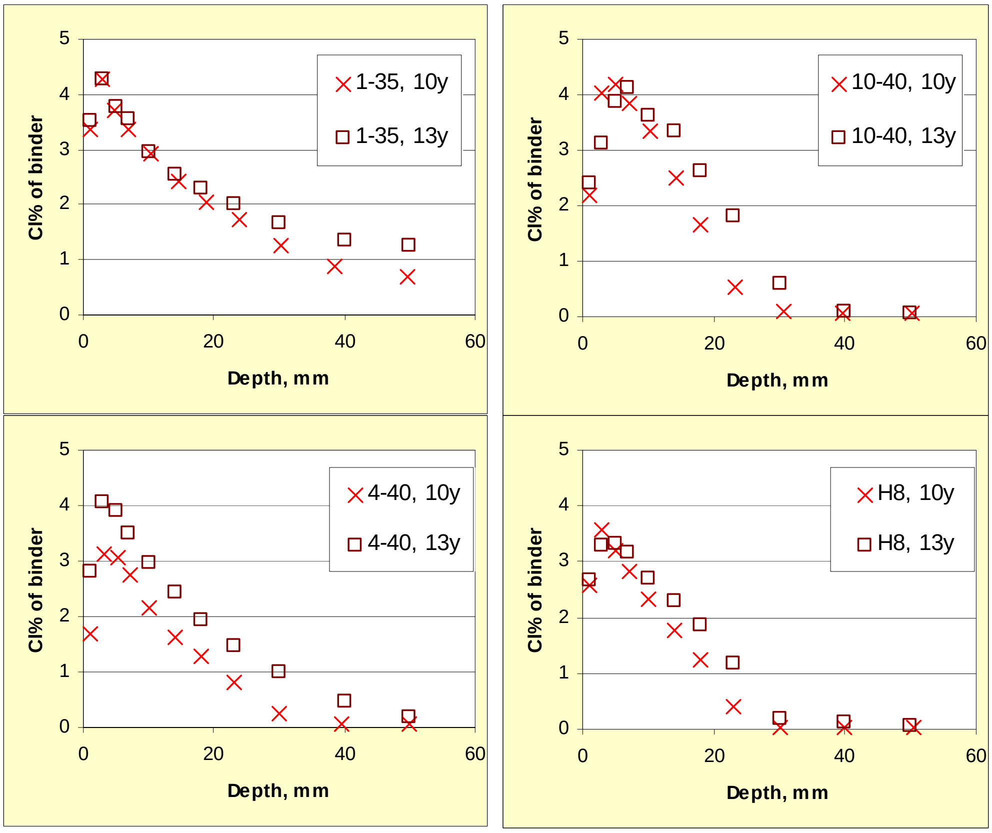

Figure 17 – Chloride penetration profiles measured after 10 and 13 years' exposure.

4.4 Relationships between corrosion and chloride

Some relationships between corrosion parameters and chloride content are shown in figures 18 and 19. Figure 18b shows that, the criteria for actual high corrosion are always related to chloride content ≥ 1% by mass of binder, despite of the types of binder. However, without destructive visual examination, it seems difficult to find clear relationships between half-cell potential or resistivity and chloride content (see figure 18 a). On the other hand, the relationship between corrosion rate and chloride content seems clearer, that is, the measured high corrosion rate is in most cases correlated to high chloride content, see figure 18a, the middle diagram. It is understandable that high chloride content may not necessarily mean high corrosion rate, but high corrosion rate should be caused by higher chloride content with regard to chloride-induced corrosion. This indicates that the non-destructive corrosion rate measurement is the most reliable parameter, while the half-cell potential and resistivity can be used as complementary parameters in the assessment of corrosion status, in supporting to the findings reported in [13]. The results from the Kristiansand slabs in figure 19 also confirmed the relationship between corrosion rate and chloride content.

Since the corrosion measurement is for the instantaneous status, the actual initiation of corrosion is unknown from this study. Therefore, the chloride level 1% by mass of binder may not be the same as the conventionally defined threshold value, but can be taken as the critical level for significant on-going corrosion that is visible by destructive visual examination.

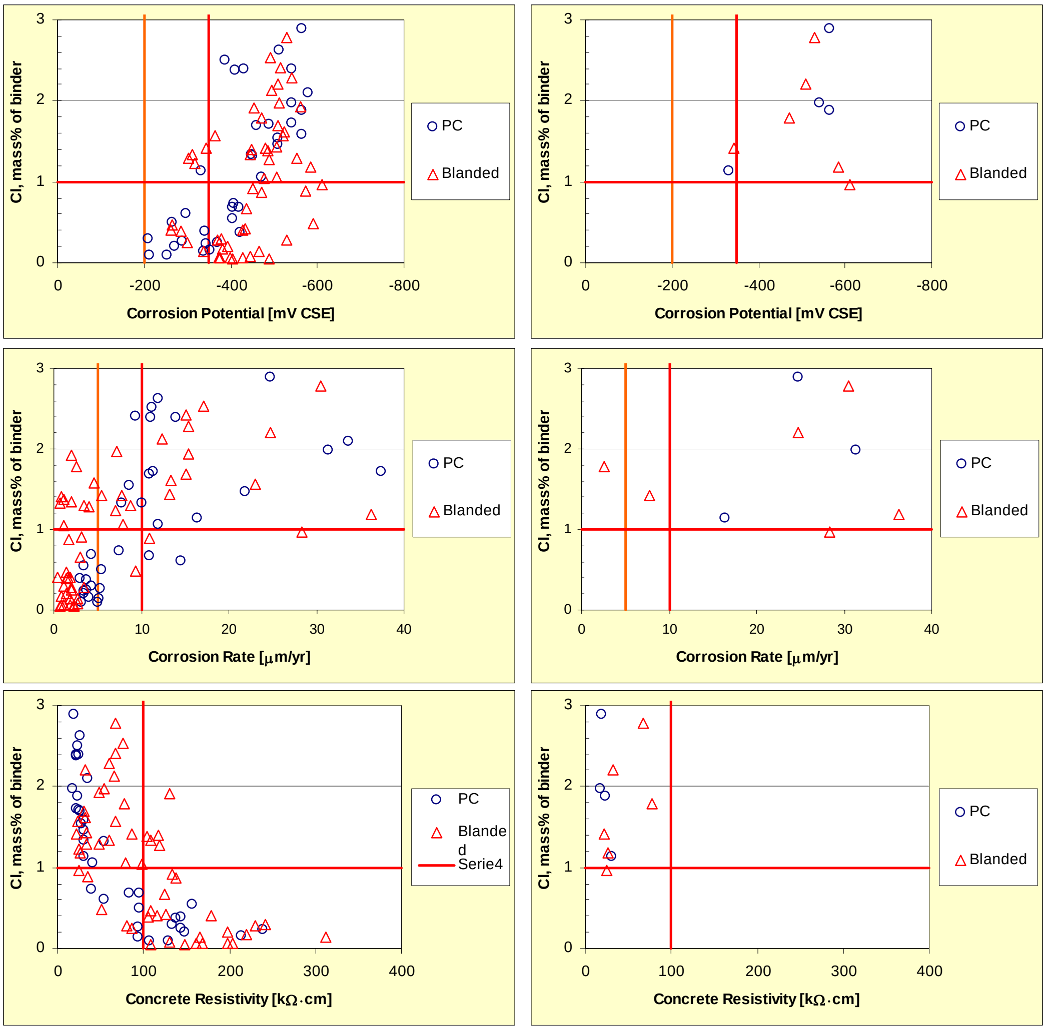

a) All measurement points

b) Points with visible corrosion

Figure 18 – Relationships between corrosion parameters and chloride content (Träslövsläge slabs).

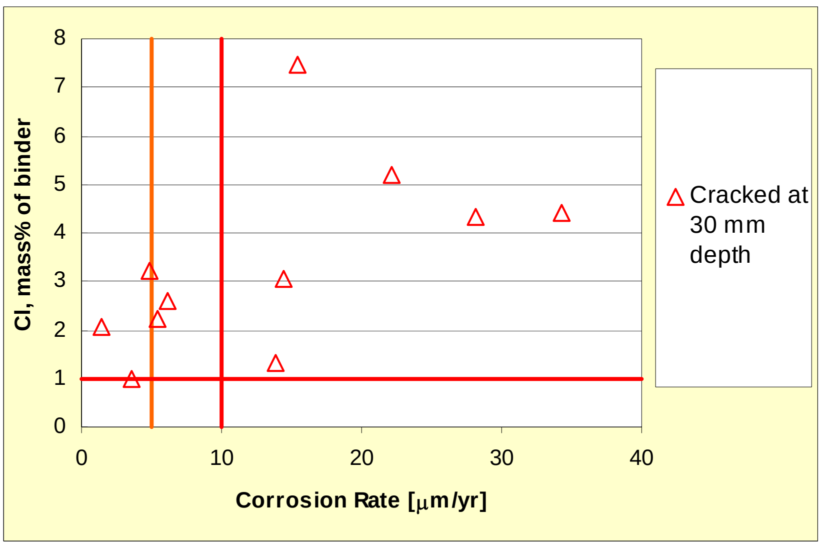

Figure 19 – Relationship between corrosion rate and chloride content (Kristiansand slabs).

5 Conclusions

Based on the findings from this study, the following conclusions may be drawn:

- The results from visual examination on about 20 rebars in 9 concrete slabs show that the newly developed rapid technique for corrosion measurement is a useful tool with reasonably good accuracy for assessment of corrosion of steel in concrete.
- The corrosion rate measurement is the most reliable parameter, while the half-cell potential and resistivity can be used as complementary parameters in the assessment of corrosion status.
- For the uncracked concrete, the visible corrosions normally occurred about 10~20 cm under the seawater level, where the oxygen may be sufficiently available for initiating the corrosion.
- As expected, for the cracked concrete, the visible corrosions occurred at the cracks.
- Chloride may easily penetrate through a poor interface between concrete and mortar spacer and initiate an early corrosion.
- Although the chloride level 1% by mass of binder may not be the same as the conventionally defined threshold value, it can be taken as the critical level for significant on-going corrosion that is visible by destructive visual examination, despite of types of binder.

As a general conclusion, thicker cover is an effective way to protect the steel from corrosion.

In production of structural concrete, measures should be taken to avoid cracks and poor interfaces, otherwise early corrosion may occur through the cracks and poor interfaces, in despite of binder type and water-binder.

References

[1] Tuutti, K., “Corrosion of Steel in Concrete”, CBI Research fo 4:82, Swedish Cement and Concrete Research Institute, Stockholm, 1982.

[2] Sandberg, P., ’Durability of concrete in saline environment’, Cementa AB, ISBN 91-87334-12-7, 1996.

[3] Sandberg, P., “Chloride initiated reinforcement corrosion in marine concrete”, PhD thesis, Lund Institute of Technology, Division of Building Materials, Report TVBM-1015, Lund, Sweden, 1998.

[4] Pettersson, K., “Corrosion threshold value and corrosion rate in reinforced concrete”, CBI Report 2:92, Stocholm, Sweden, 1992.

[5] Pettersson, K., “Service life of concrete structures – in a chloride environment”, CBI Report 1:97, Stocholm, Sweden, 1997.

[6] Tang, L., “Chloride Transport in Concrete – Measurement and Prediction”, PhD thesis, Chalmers University of Technology, Dept. of Building Materials, Publication P-96:6, Gothenburg, Sweden, 1996.

[7] Pettersson, K., “Corrosion of steel in high performance concrete - A literature review”, CBI, internal report, 11 pp, Sept. 1992.

[8] Cementa et al, “Betonghandbok Högpresterande betong – Material och utförande”, AB Svensk Byggtjänst, Stockholm 2000. 419pp.

[9] Tang L., “Mapping Corrosion of Steel in Reinforced Concrete Structures”, SP RAPPORT 2002:32, SP Sveriges Provnings- och Forskningsinstitut, Borås, 2002.

[10] Tang, L., “A rapid technique for detecting corrosion of steel in reinforced concrete”, Proceedings of International Conference on Concrete Repair, Rehabilitation and Retrofitting, Cape Town, South Africa, 21-23 November 2005, pp. 375-381.

[11] Tang, L., “Calibration of the Electrochemical Methods for the Corrosion Rate Measurement of Steel in Concrete - Nordtest project No. 1531-01”. SP Report 2002:25, Borås: SP Swedish National Testing and Research Institute.

[12] Tang, L., “Chloride Ingress in Concrete Exposed to Marine Environment – Field data up to 10 years’ exposure”, SP Report 2003:16, SP Swedish National Testing and Research Institute, Borås, Sweden, 2003.

[13] Tang, L. & Malmberg, B., “Assessment of Reinforcement Corrosion in Concrete Highway Tunnel Structures”, accepted for publication in Proceedings of International Conference on Concrete Repair, Rehabilitation and Retrofitting, Cape Town, South Africa, 21-23 November 2005, pp. 409-414.

Slab No.	Steel	Diameter mm	Cover mm	Half-cell potential mV[CSE]	Corrosion rate µm/yr	Resistivitet kΩ.cm	Type of binder	w/b	Corrosion Risk
H2	Rebar 1	20	15	-414	5.1	248	90%Anl.+10%SF	0.3	3
	Stainless	20	20	-99	0.7	138			1
	Rebar 2	20	20	-453	4.8	164			2
8-35	Rebar 1	20	15	-297	3.4	150	100%Slite	0.35	2
	Stainless	20	20	-252	0.7	107			1
	Rebar 2	20	15	-467	8.2	81			3
H5	Rebar 1	20	15	-560	2.1	84	95%Anl.+5%SF	0.25	2
	Stainless	20	20	-228	0.7	121			1
	Rebar 2	20	20	-557	11.8	84			4
H6	Rebar 1	20	20	-462	3.1	151	95%Anl.+5%FA	0.3	2
	Stainless	20	20	-85	0.5	110			1
	Rebar 2	20	15	-466	9.8	133			3
11-35	Rebar 1	20	20	-429	5.1	84	85%DK+10%FA+5%SF	0.35	3
	Stainless	20	20	-170	0.8	77			1
	Rebar 2	20	15	-481	1.9	68			2
3-402	Rebar 1	20	35	-218	4.9	32	95%Anl.+5%SF	0.4	1
	Stainless	20	50	-68	1	36			1
	Rebar 2	20	50	-185	2.7	54			1
3-402V	Rebar 1	12	10	-407	4.8	153	95%Anl.+5%SF	0.4	2
	Stainless	12	10	-112	0.6	133			1
	Rebar 2	12	15	-432	1.6	170			2
2-401	Rebar 1	12	10	-497	2.5	185	100%Slite	0.4	2
	Stainless	12	15	-143	2.2	102			1
	Rebar 2	12	15	-479	5	131			2
11-35	Rebar 1	12	15	-365	1.1	147	85%DK+10%FA+5%SF	0.35	2
	Stainless	12	15	-426	0.5	173			1
	Rebar 2	12	10	-431	4.7	300			2
3-352	Rebar 1	20	40	-68	1.1	112	95%Anl.+5%SF	0.35	1
	Stainless	20	50	-41	0	286			1
	Rebar 2	20	55	-26	2.4	101			1
2-352	Rebar 1	20	40	-122	3.9	103	100%Slite	0.35	1
	Stainless	20	50	-129	0.7	113			1
	Rebar 2	20	55	-144	1.9	91			1
1-402	Rebar 1	20	50	-296	4	85	100%Anl.	0.4	2
	Stainless	20	50	-175	1.5	86			1
	Rebar 2	20	40	-296	2	133			2
3-351	Rebar 1	20	20	-326	2.6	221	95%Anl.+5%SF	0.35	2
	Stainless	20	20	-69	0.9	75			1
	Rebar 2	20	15	-325	4.5	317			2
8-40	Rebar 1	20	15	-441	2	150	100%Slite	0.4	2
	Stainless	20	20	-65	0.7	87			1
	Rebar 2	20	20	-333	3	159			2
H9	Rebar 1	20	15	-475	4	230	100%Deg400	0.3	2
	Stainless	20	20	-284	1	146			1
	Rebar 2	20	20	-508	5.9	128			3
H1	Rebar 1	12	10	-477	5.4	261	95%Anl.+5%SF	0.3	3
	Stainless	12	15	-139	1.1	146			1
	Rebar 2	12	20	-466	4.3	130			2
H3	Rebar 1	12	15	-448	2.8	161	100%Anl.	0.3	2
	Stainless	12	15	-104	1.1	147			1
	Rebar 2	12	10	-432	3.5	325			2
H3	Rebar 1	12	35	-103	4.8	97	100%Anl.	0.3	1
	Stainless	12	30	-93	2.2	84			1
	Rebar 2	12	30	-57	3.5	104			1
H3	Rebar 1	12	60	-201	2.2	47	100%Anl.	0.3	1
	Stainless	12	60	-176	0.5	51			1
	Rebar 2	12	60	-189	2.4	35			1
8-50	Rebar 1	12	10	-517	7.3	140	100%Slite	0.5	3
	Stainless	12	15	-151	0.7	97			1
	Rebar 2	12	15	-515	5.2	109			3
H9	Rebar 1	12	15	-186	1.9	192	100%Deg400	0.3	1
	Stainless	12	15	-72	0.9	223			1
	Rebar 2	12	10	-317	3.6	217			2
1-402	Rebar 1	20	15	-521	6.4	109	100%Anl.	0.4	3
	Rebar 2	20	20	-512	2.4	92			2
	Rebar 1, At	20	15	-321	2.7	230			2
	Rebar 2, At	20	20	-301	2.3	221			2
3-352	Rebar 1	12	10	-310	1.3	312	95%Anl.+5%SF	0.35	2
	Rebar 2	12	15	-496	4.4	283			2
1-351	Rebar 1	12	10	-488	3.9	293	100%Anl.	0.35	2
	Rebar 2	12	15	-360	3.7	196			2
1-402	Rebar 1	12	15	-505	3.6	244	100%Anl.	0.4	2

Slab No.	Steel	Diameter mm	Cover mm	Half-cell potential mV[CSE]	Corrosion rate µm/yr	Resistivitet kΩ.cm	Type of binder	w/b	Corrosion Risk
	Rebar 2	12	10	-490	3.5	319			2
12-35	Rebar 1	12	10	-315	6.4	281	85%Anl.+10%FA+5%SF	0.35	3
	Rebar 2	12	15	-303	4.4	131			2
H2	Rebar 1	12	30	-81	1.2	190	90%Anl.+10%SF	0.3	1
	Rebar 2	12	30	-45	2.8	174			1
H5	Rebar 1	12	30	-86	2.7	126	95%Anl.+5%SF	0.25	1
	Rebar 2	12	30	-57	4.8	218			1
H2	Rebar 1	12	30	-170	3.4	102	90%Anl.+10%SF	0.3	1
	Rebar 2	12	30	-105	4.1	110			1
2-50	Rebar 1	12	10	-527	10.6	147	100%Slite	0.5	4
	Rebar 2	12	15	-323	5.2	113			3
2-35	Rebar 1	20	20	-550	22.1	60	100%Slite	0.35	4
	Rebar 2	20	20	-540	21.5	26			4
8-35	Rebar 1	12	20	-532	2.8	98	100%Slite	0.35	2
	Rebar 2	12	15	-400	1.8	183			2
7-40	Rebar 1	12	10	-493	5.4	210	100%Anl.	0.4	3
	Rebar 2	12	15	-266	4.9	270			2
6-35	Rebar 1	20	25	-198	0	460	95%Anl.+5%SF	0.35	1
	Rebar 2	20	20	-397	2.1	279			2
6-40	Rebar 1	20	15	-379	2	444	95%Anl.+5%SF	0.4	2
	Rebar 2	20	20	-407	2.1	314			2
4-40	Rebar 1	20	20	-404	3.5	345	90%Anl.+10%SF	0.4	2
	Rebar 2	20	15	-487	6.1	294			3
5-40	Rebar 1	20	15	-362	1.5	328	95%Anl.+5%SF	0.4	2
	Rebar 2	20	20	-340	1.4	354			2
10-40	Rebar 1, Su	12	15	-492	5.9	83	78.5%DK+17%FA+4.5%SF	0.4	3
	Rebar 2, Su	12	10	-593	24.4	54			4
	Rebar 1	12	15	-406	0.7	157			1
	Rebar 2	12	10	-506	0.8	170			1
1-352	Rebar 1, Su	20	20	-533	28.5	33	100%Anl.	0.35	4
	Rebar 2, Su	20	15	-542	26.2	27			4
	Rebar 2	20	15	-457	23	98			4
	Rebar 1	20	20	-471	16.4	59			4
H5	Rebar 1	12	35	-136	4.6	62	95%Anl.+5%SF	0.25	1
	Rebar 2	12	35	-177	3.4	72			1
H8	Rebar 1	12	15	-574	22.2	33	80%Anl.+20%FA	0.3	4
	Rebar 2	12	10	-546	8.9	64			3
4-40	Rebar 1	12	15	-531	22.4	16	90%Anl.+10%SF	0.4	4
	Rebar 2	12	15	-340	2.5	20			2
7-35	Rebar 1	20	20	-558	7.5	71	100%Anl.	0.35	3
	Rebar 2	20	15	-581	4.1	35			2
H7	Rebar 1	20	10	-502	9.6	253	95%Deg400+5%SF	0.3	3
	Rebar 2	20	15	-166	2.9	156			1

Remarks

1	No or negligible corrosion
2	Low corrosion
3	Moderate corrosion
4	High corrosion

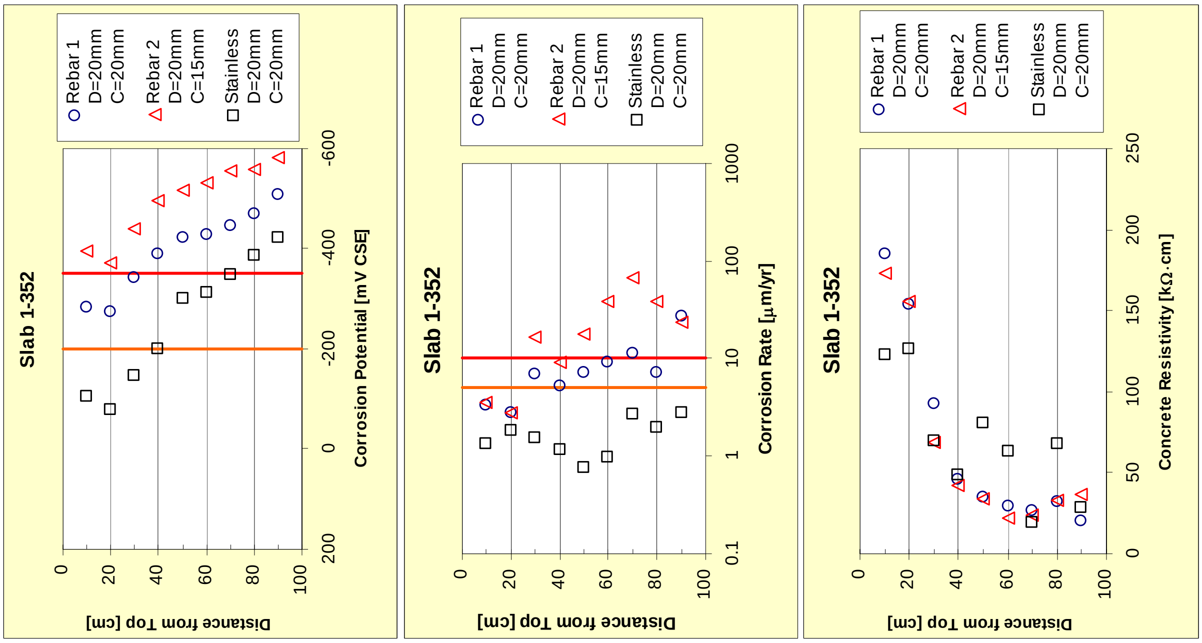

Measured on 21 June 2005

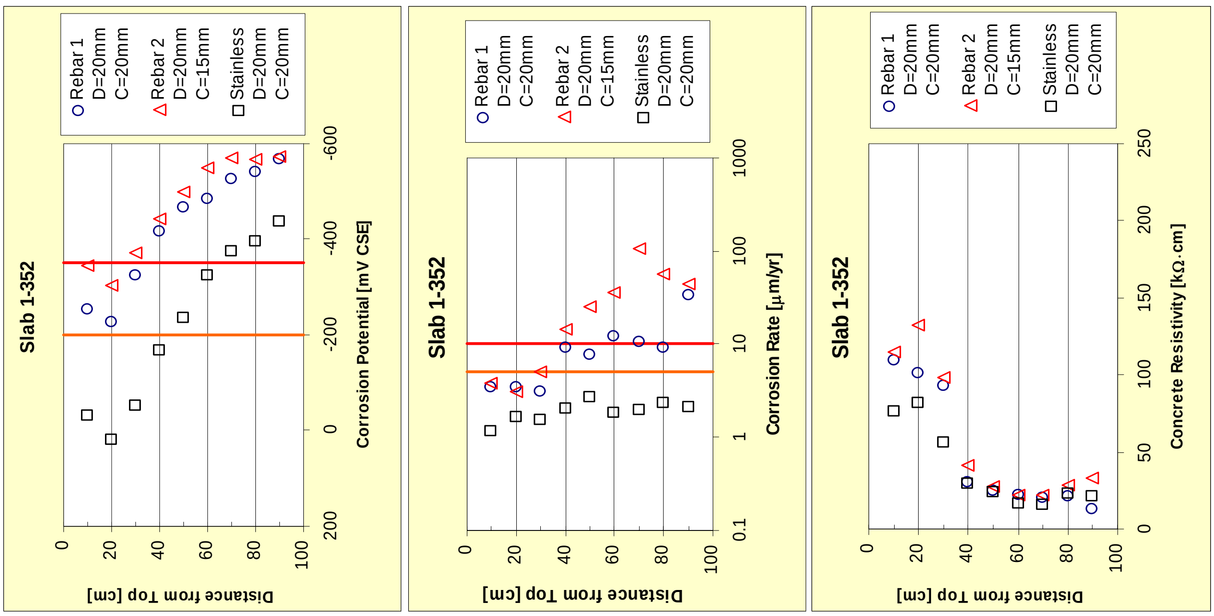

Measured on 16 June 2005

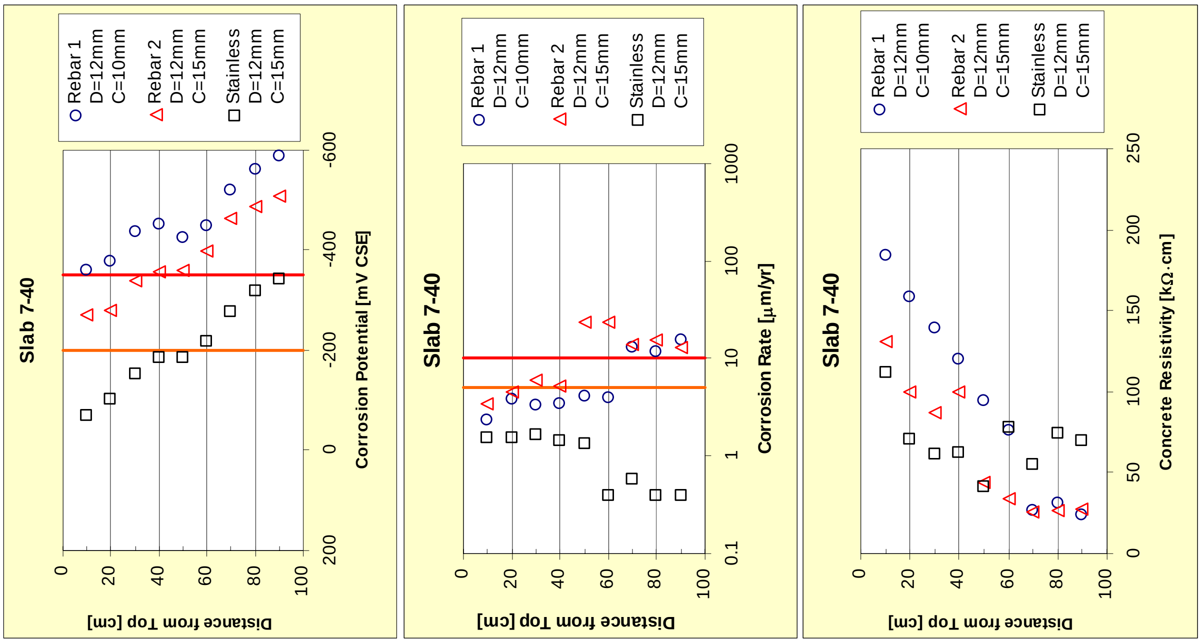

Measured on 21 June 2005

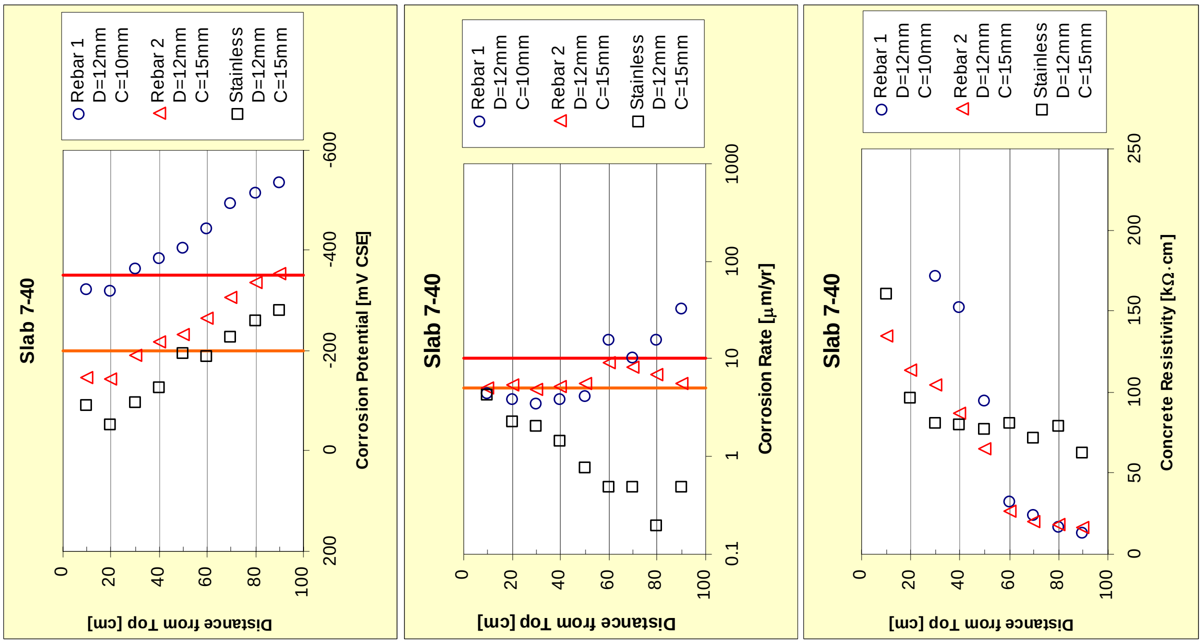

Measured on 16 June 2005

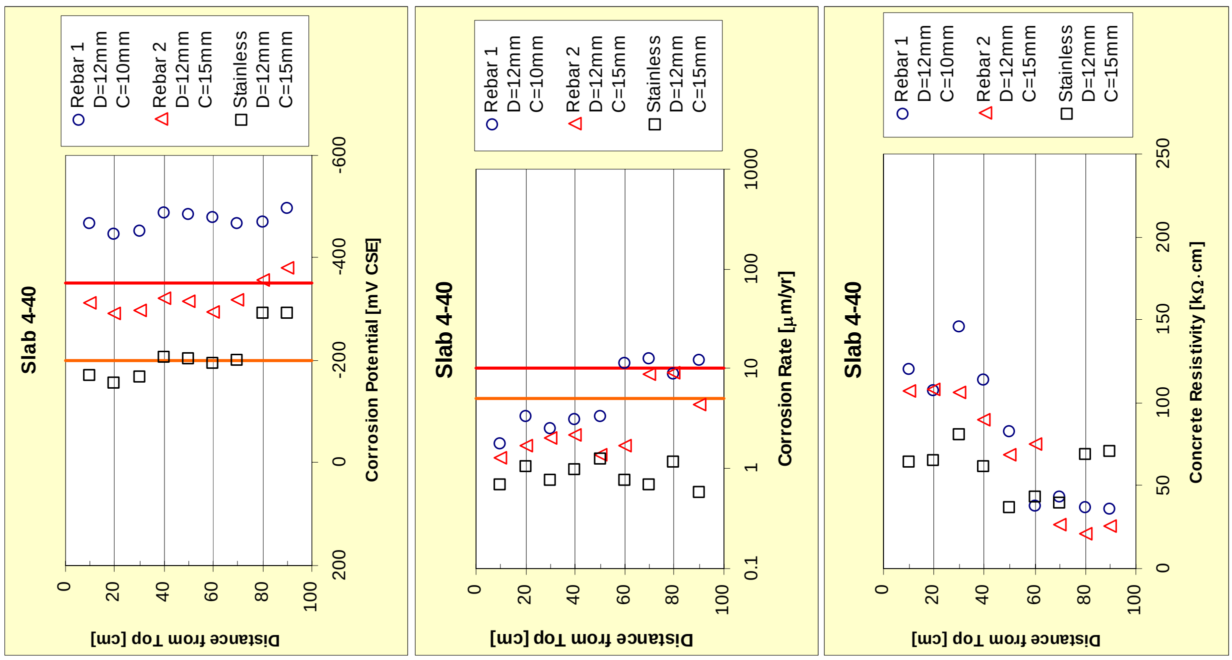

Measured on 21 June 2005

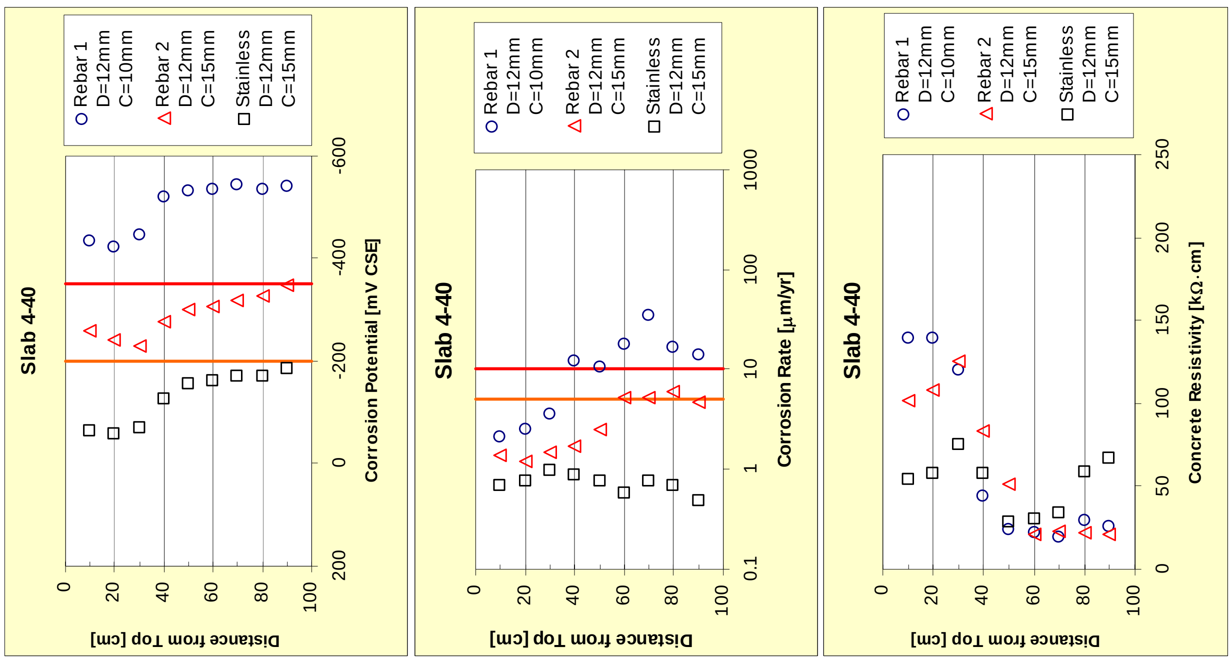

Measured on 16 June 2005

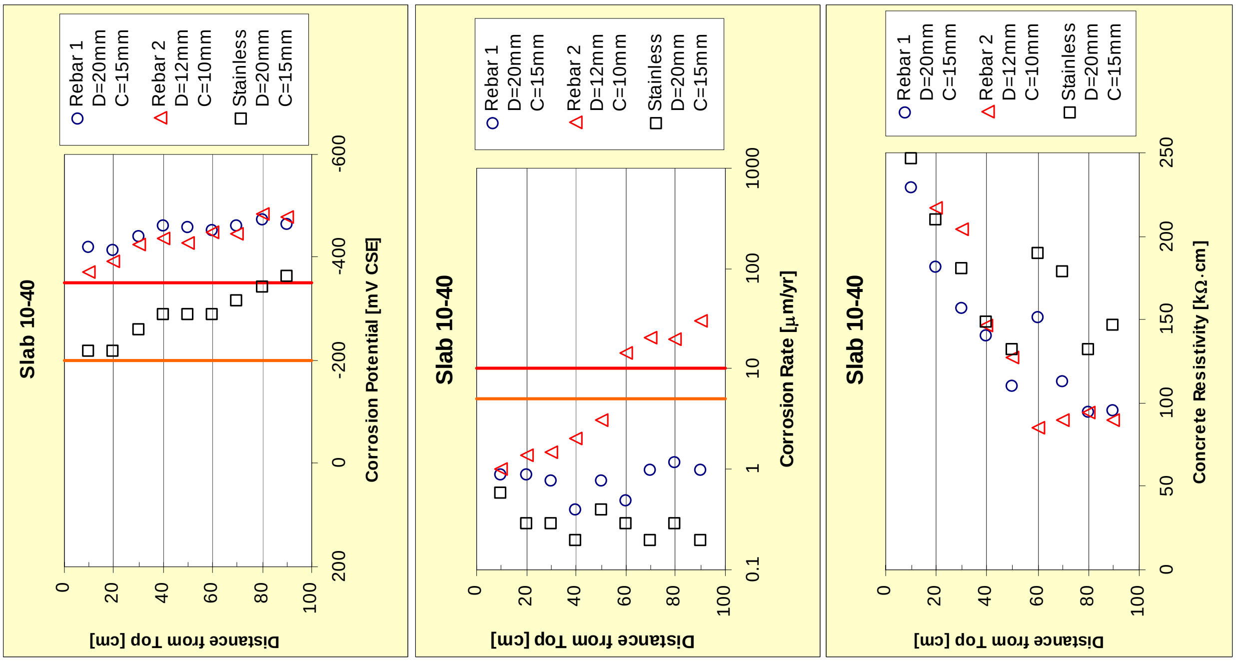

Measured on 21 June 2005

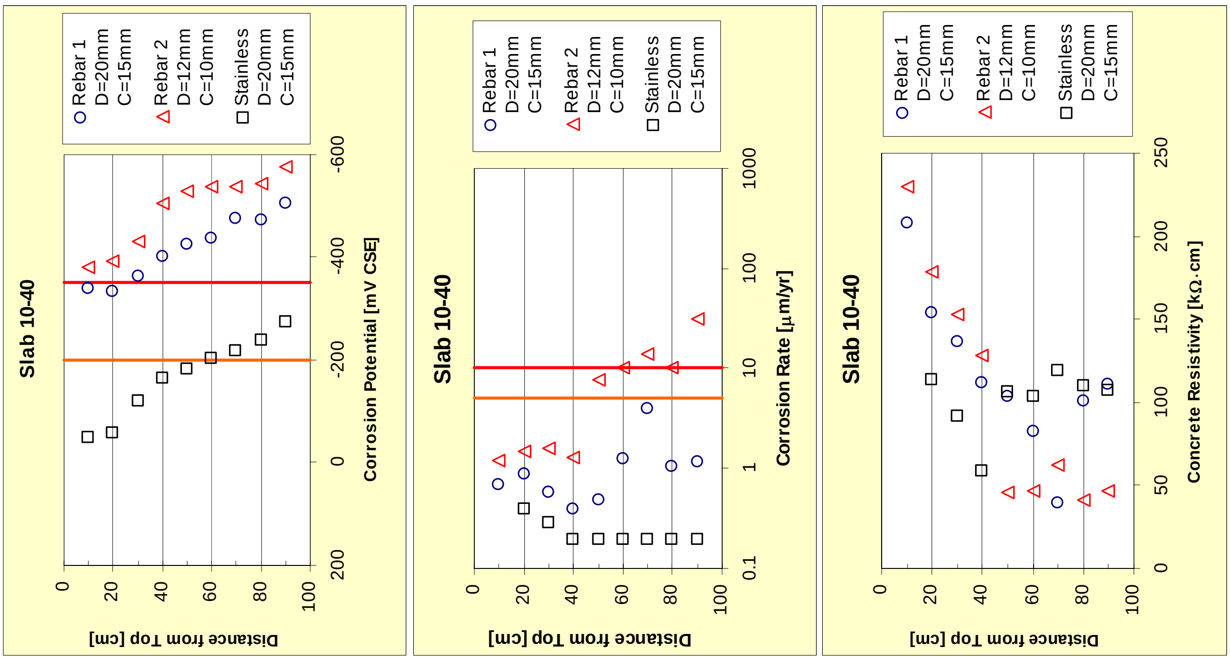

Measured on 16 June 2005

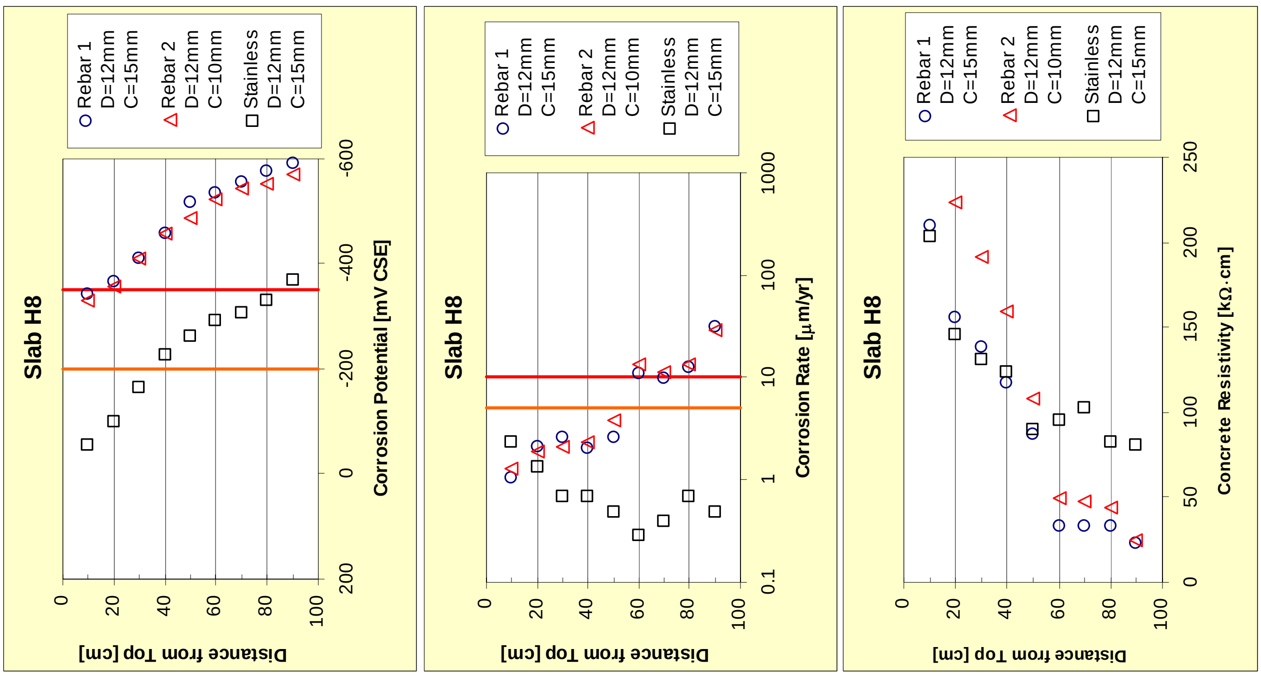

Measured on 16 June 2005

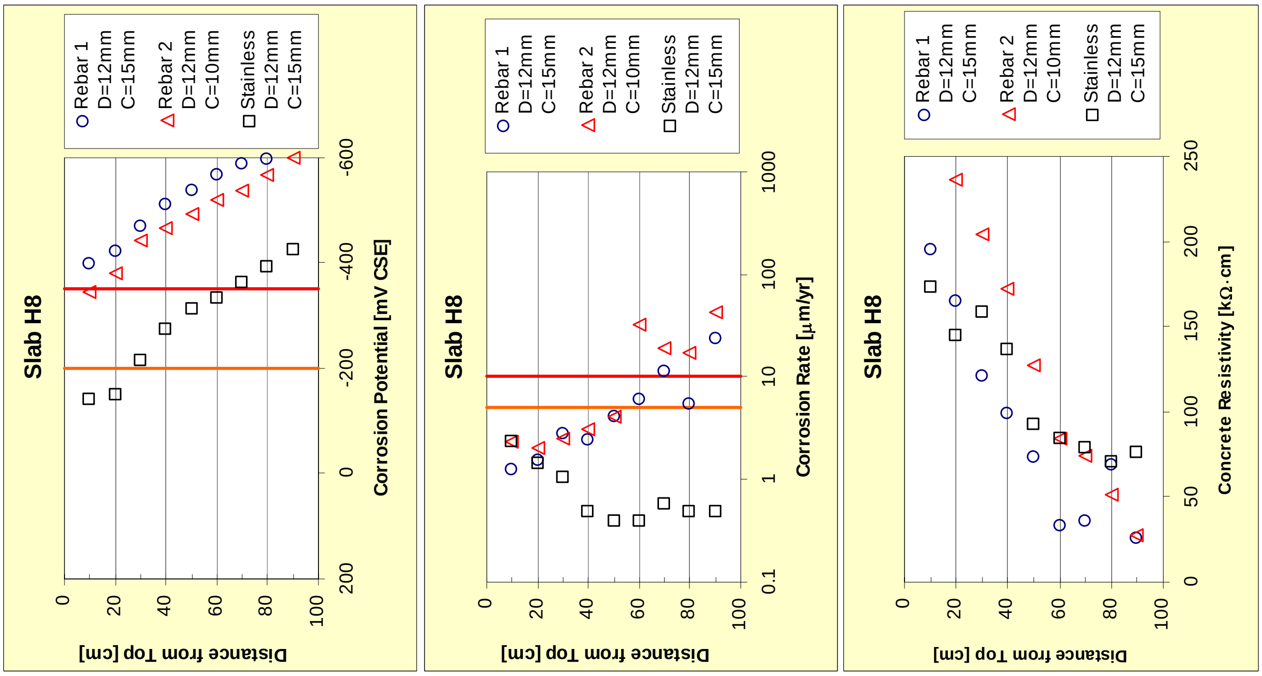

Measured on 21 June 2005

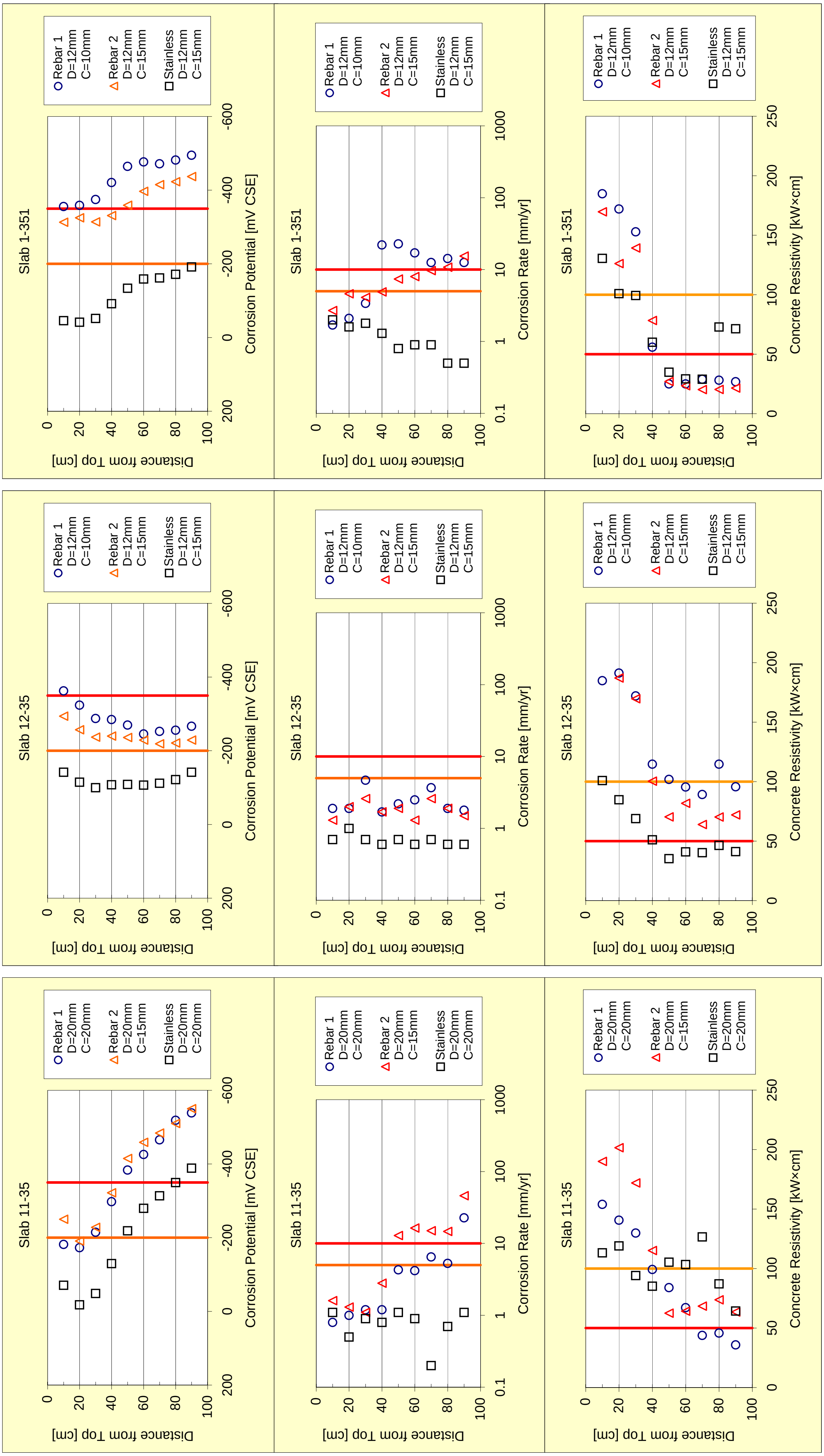
Slab 1-351
Slab 12-35
Slab 11-35
Distance from Top [cm]
Corrosion Potential [mV CSE]
Corrosion Rate [mm/yr]
Concrete Resistivity [kW×cm]
Rebar 1 D=12mm C=10mm
Rebar 2 D=12mm C=15mm
Stainless D=12mm C=15mm
Rebar 1 D=20mm C=20mm
Rebar 2 D=20mm C=15mm
Stainless D=20mm C=20mm

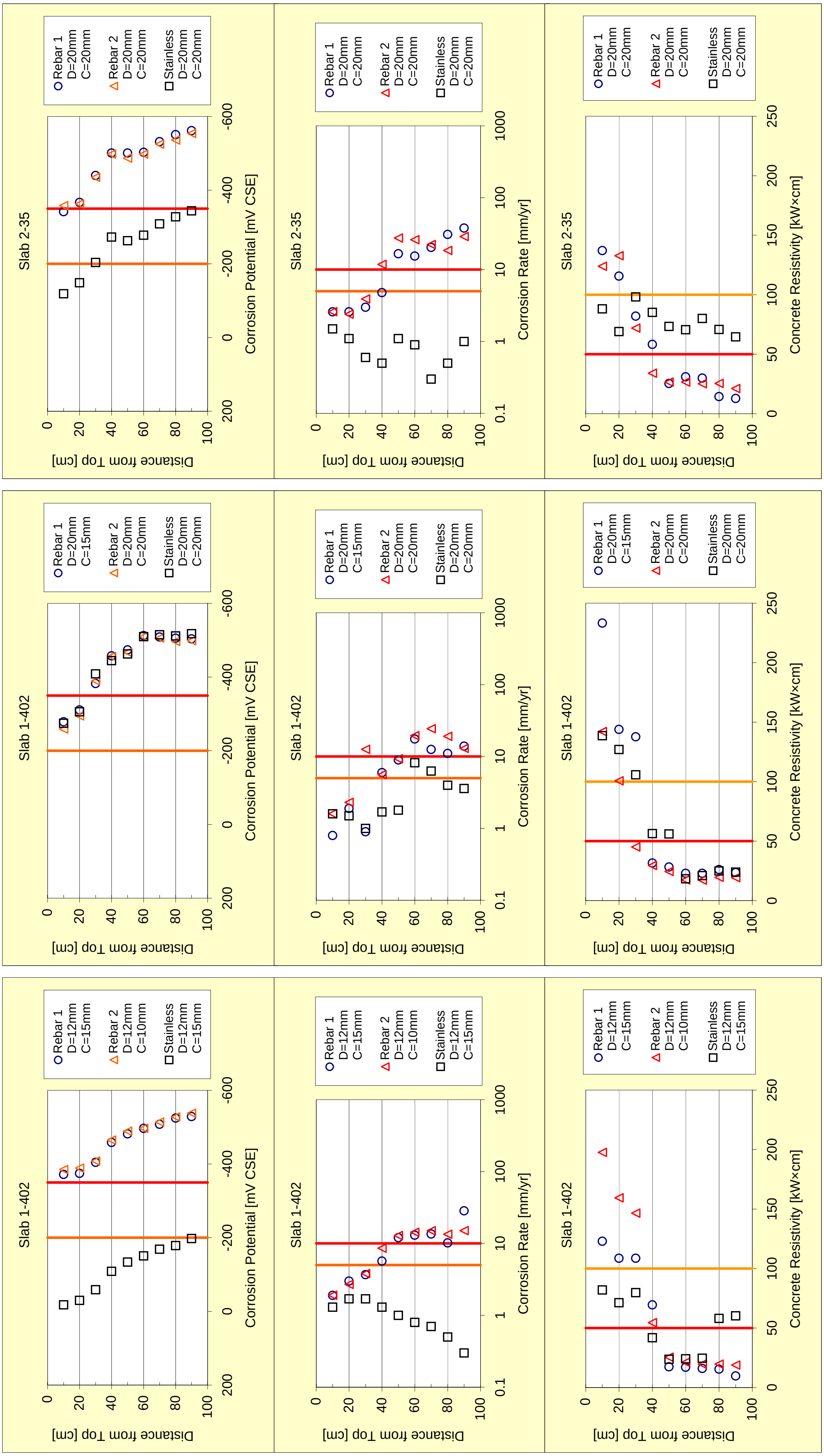
Slab 2-35
Slab 1-402
Slab 1-402
Rebar 1 D=20mm C=20mm
Rebar 2 D=20mm C=20mm
Stainless D=20mm C=20mm
Rebar 1 D=20mm C=15mm
Rebar 1 D=12mm C=15mm
Rebar 2 D=12mm C=10mm
Stainless D=12mm C=15mm
Distance from Top [cm]
Corrosion Potential [mV CSE]
Corrosion Rate [mm/yr]
Concrete Resistivity [kW×cm]

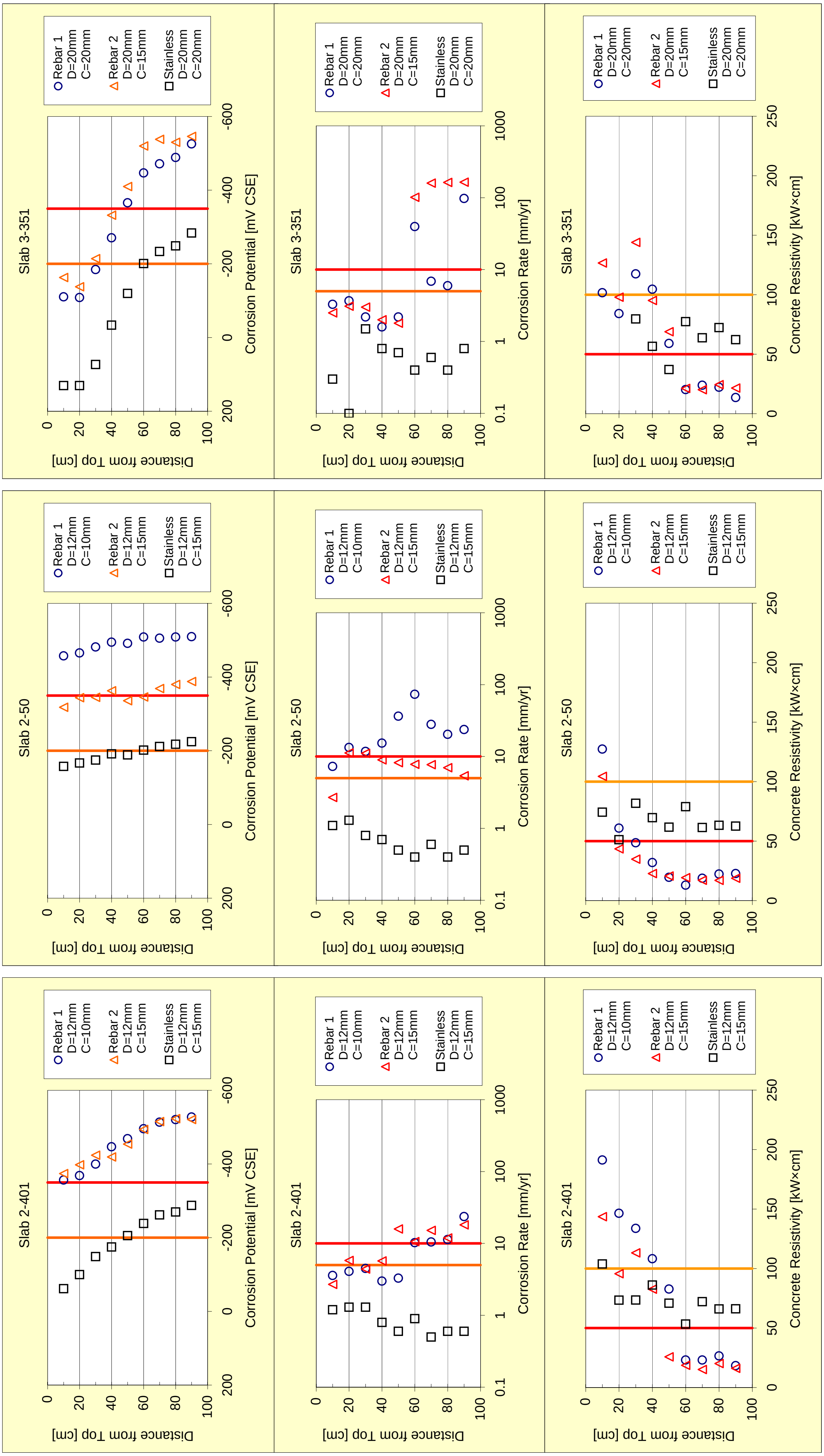
Slab 3-351
Slab 2-50
Slab 2-401
Distance from Top [cm]
Corrosion Potential [mV CSE]
Corrosion Rate [mm/yr]
Concrete Resistivity [kW×cm]
Rebar 1 D=20mm C=20mm
Rebar 2 D=20mm C=15mm
Stainless D=20mm C=20mm
Rebar 1 D=12mm C=10mm
Rebar 2 D=12mm C=15mm
Stainless D=12mm C=15mm

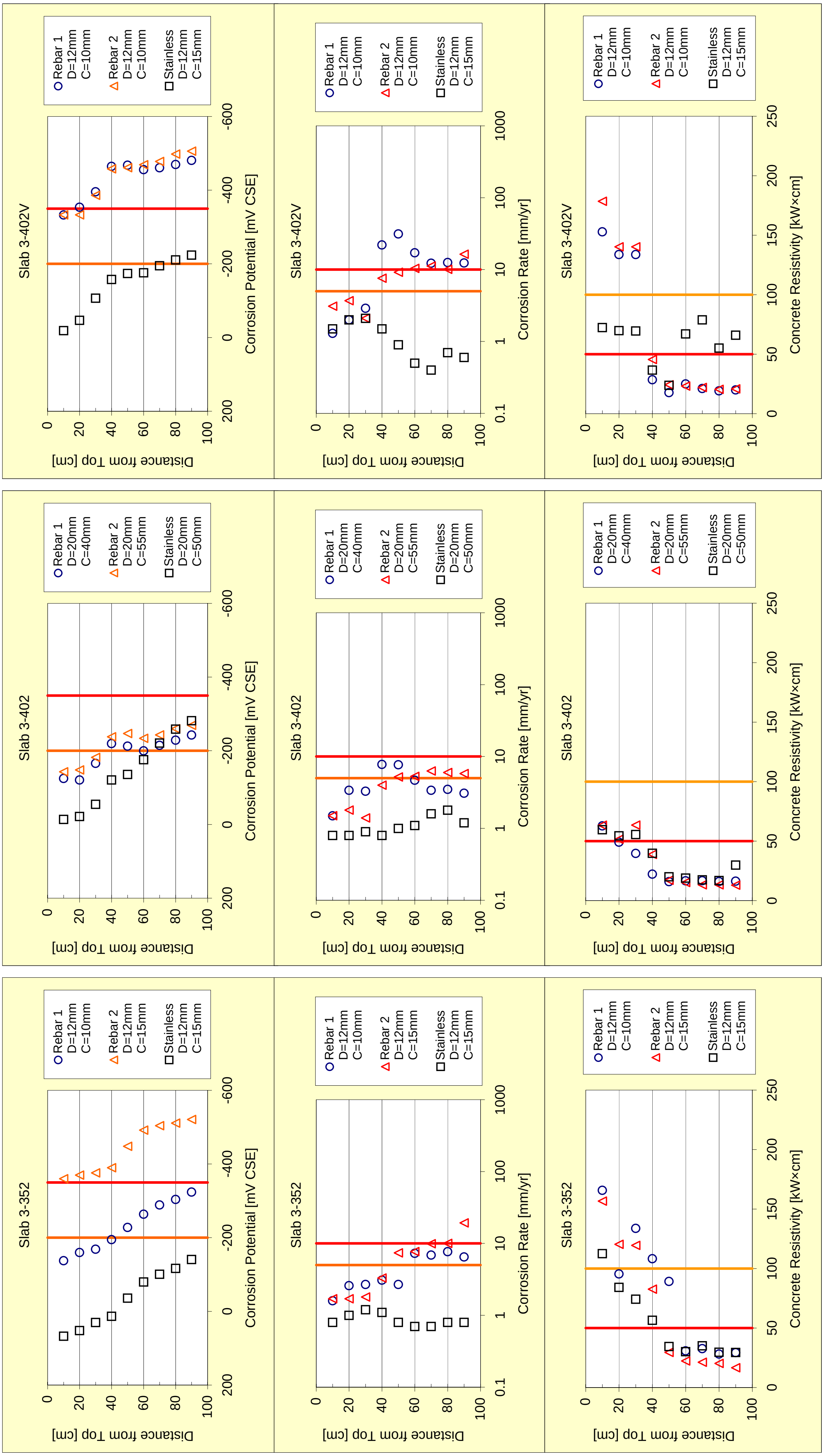
Slab 3-402V
Slab 3-402
Slab 3-352
Distance from Top [cm]
Corrosion Potential [mV CSE]
Corrosion Rate [mm/yr]
Concrete Resistivity [kW×cm]
Rebar 1 D=12mm C=10mm
Rebar 2 D=12mm C=10mm
Stainless D=12mm C=15mm
Rebar 1 D=20mm C=40mm
Rebar 2 D=20mm C=55mm
Stainless D=20mm C=50mm
Rebar 1 D=12mm C=10mm
Rebar 2 D=12mm C=15mm
Stainless D=12mm C=15mm

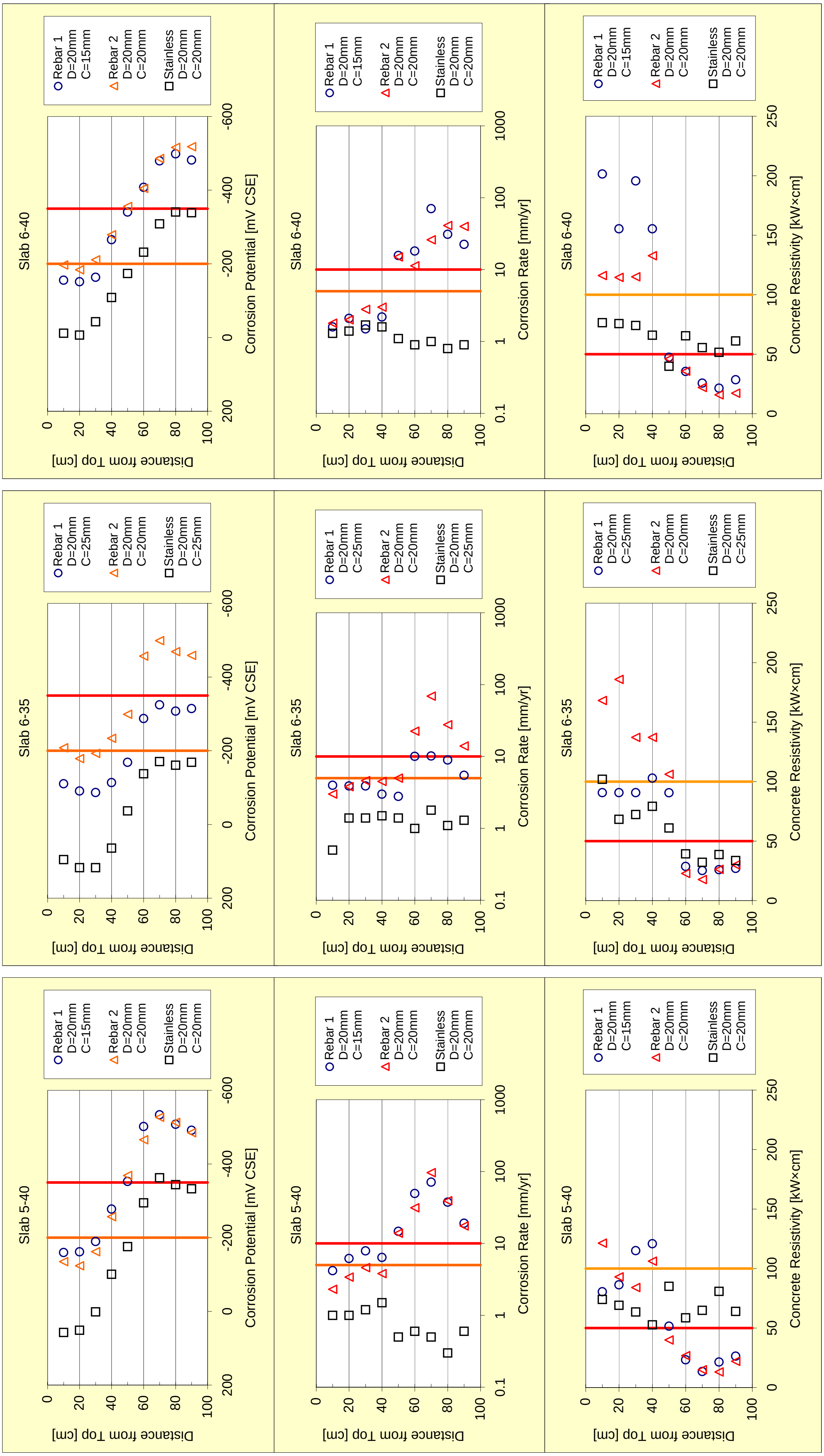
Slab 6-40
Slab 6-35
Slab 5-40
Rebar 1 D=20mm C=15mm
Rebar 2 D=20mm C=20mm
Stainless D=20mm C=20mm
Rebar 1 D=20mm C=25mm
Stainless D=20mm C=25mm
Distance from Top [cm]
Corrosion Potential [mV CSE]
Corrosion Rate [mm/yr]
Concrete Resistivity [kW×cm]

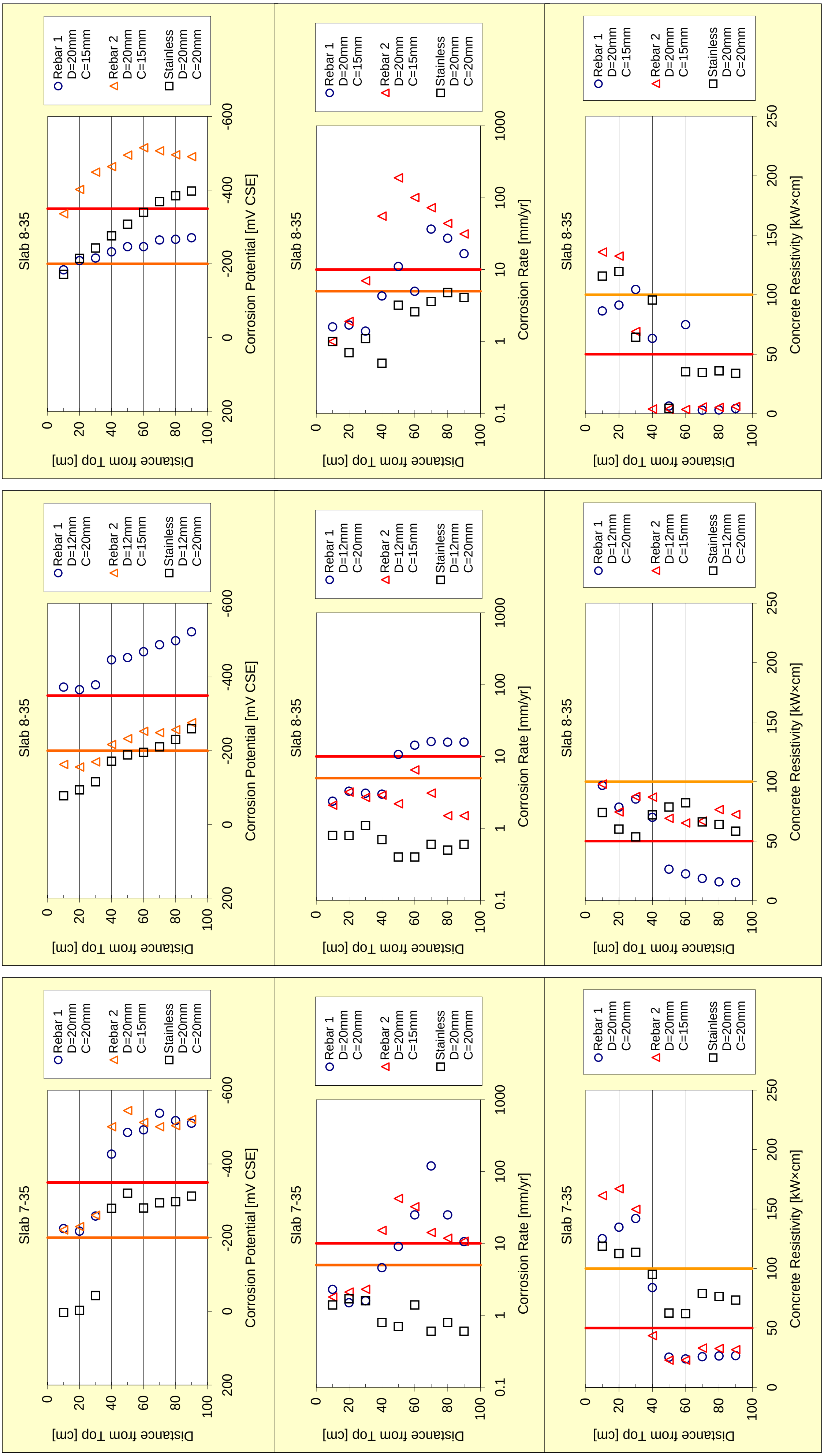
Slab 7-35
Slab 8-35
Distance from Top [cm]
Corrosion Potential [mV CSE]
Corrosion Rate [mm/yr]
Concrete Resistivity [kW×cm]
Rebar 1 D=20mm C=20mm
Rebar 2 D=20mm C=15mm
Stainless D=20mm C=20mm
Rebar 1 D=12mm C=20mm
Rebar 2 D=12mm C=15mm
Stainless D=12mm C=20mm
Rebar 1 D=20mm C=15mm

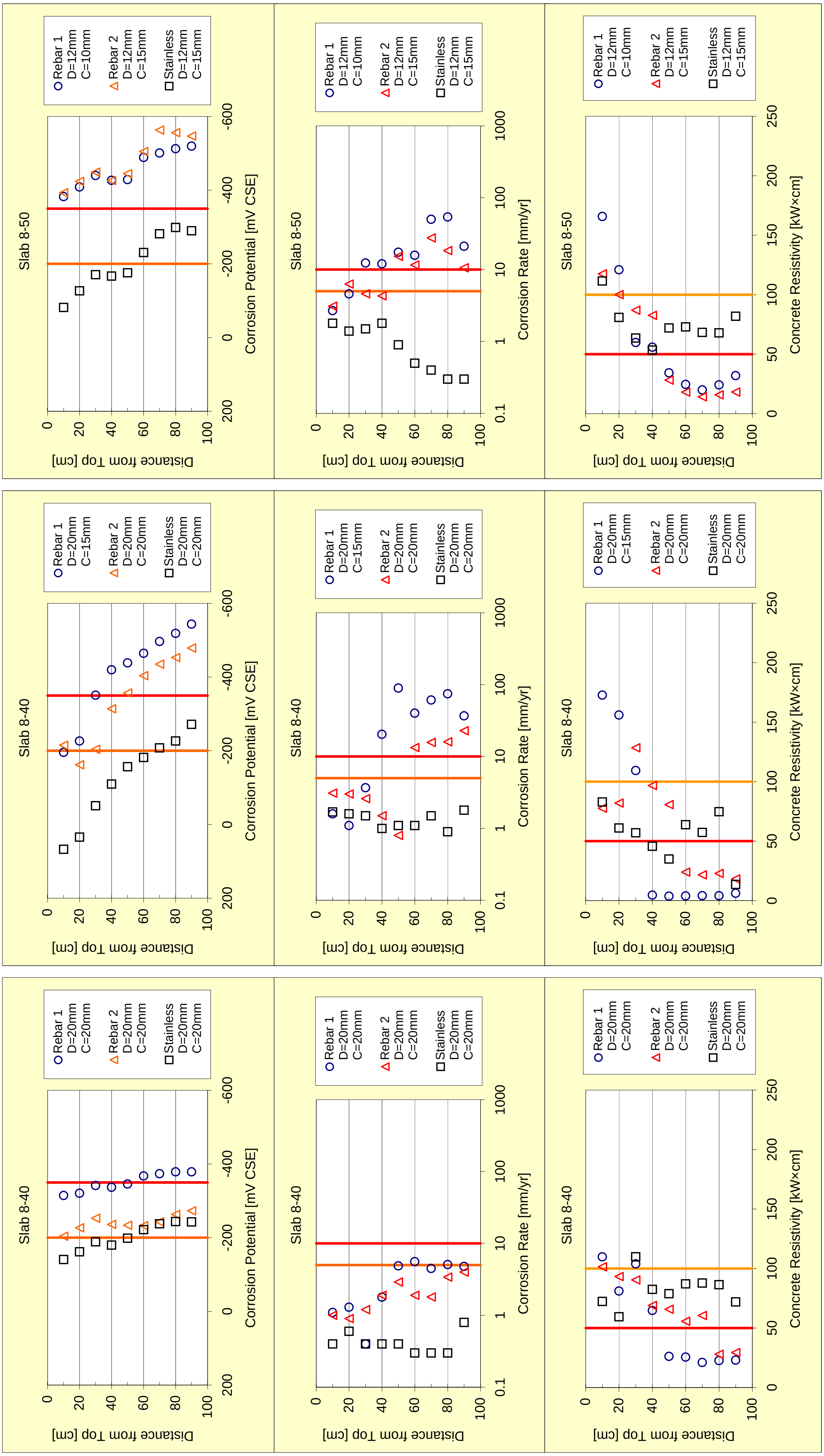
Slab 8-50
Slab 8-40
Slab 8-40
Distance from Top [cm]
Corrosion Potential [mV CSE]
Corrosion Rate [mm/yr]
Concrete Resistivity [kW×cm]
Rebar 1 D=12mm C=10mm
Rebar 2 D=12mm C=15mm
Stainless D=12mm C=15mm
Rebar 1 D=20mm C=15mm
Rebar 2 D=20mm C=20mm
Stainless D=20mm C=20mm
Rebar 1 D=20mm C=20mm
Rebar 2 D=20mm C=20mm
Stainless D=20mm C=20mm

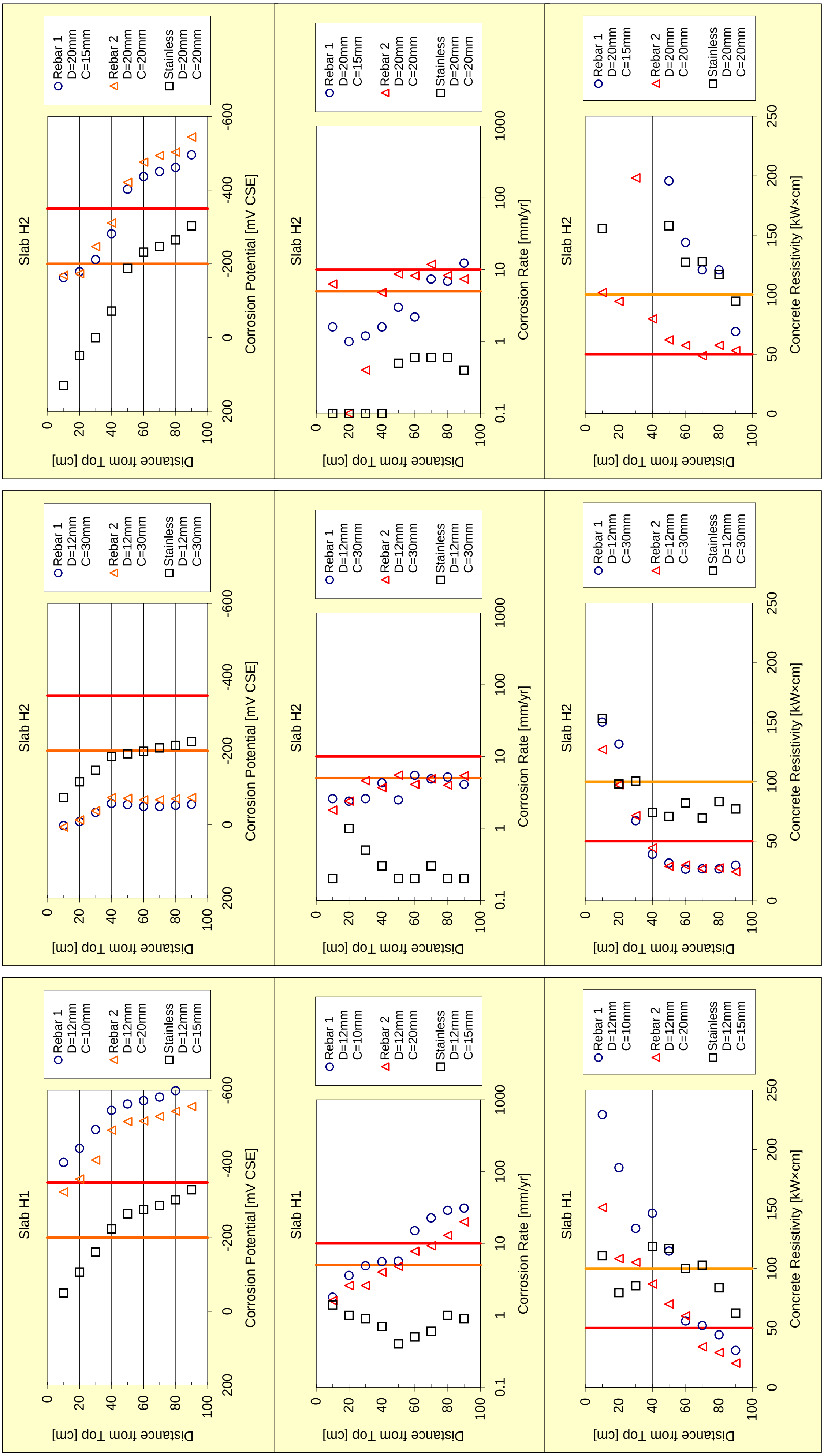
Slab H1
Slab H2
Slab H2
Corrosion Potential [mV CSE]
Corrosion Rate [mm/yr]
Concrete Resistivity [kW×cm]
Distance from Top [cm]
Rebar 1 D=12mm C=10mm
Rebar 2 D=12mm C=20mm
Stainless D=12mm C=15mm
Rebar 1 D=12mm C=30mm
Rebar 2 D=12mm C=30mm
Stainless D=12mm C=30mm
Rebar 1 D=20mm C=15mm
Rebar 2 D=20mm C=20mm
Stainless D=20mm C=20mm

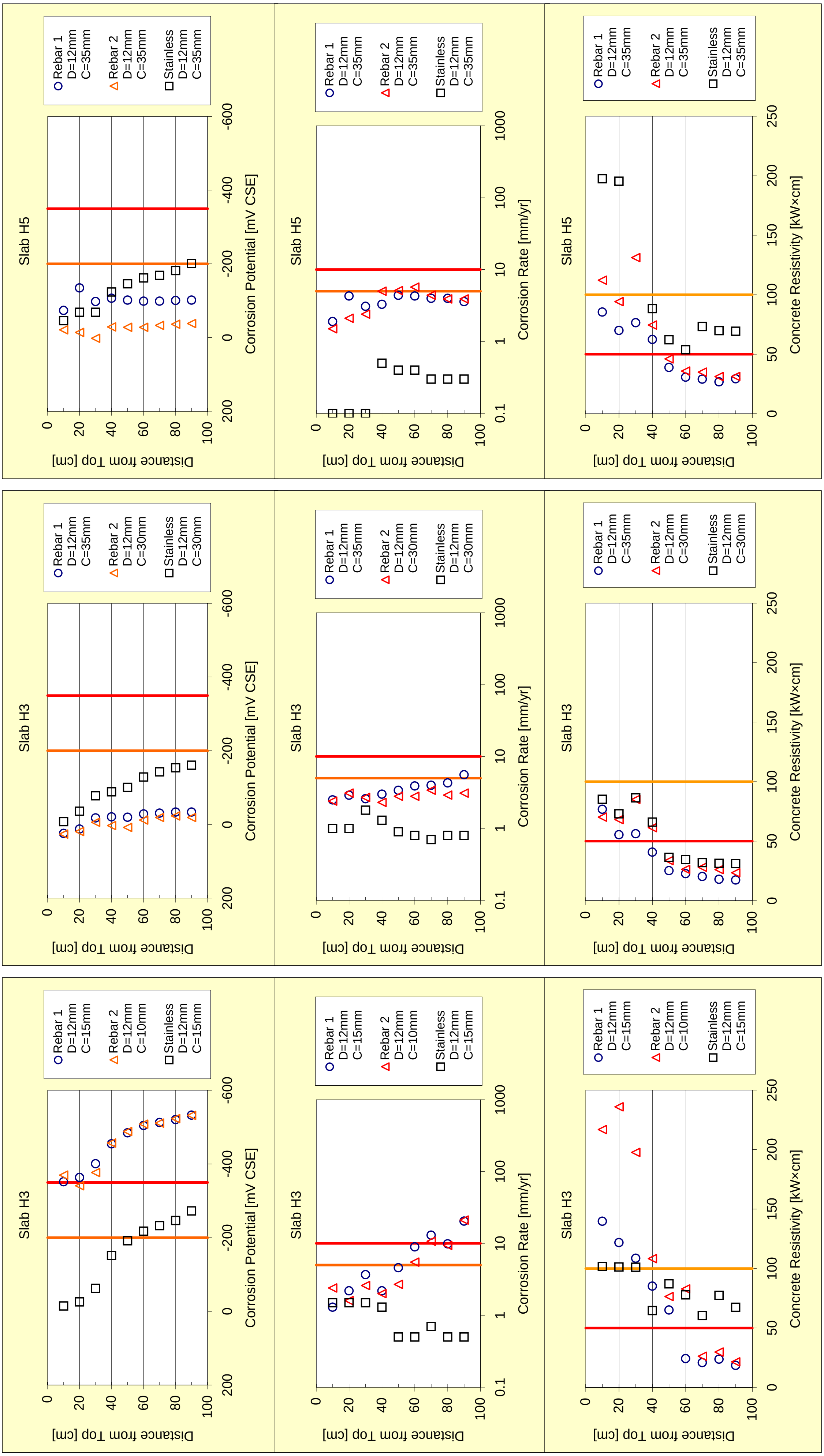
Slab H5
Slab H3
Slab H3
Distance from Top [cm]
Corrosion Potential [mV CSE]
Corrosion Rate [mm/yr]
Concrete Resistivity [kW×cm]
Rebar 1 D=12mm C=35mm
Rebar 2 D=12mm C=35mm
Stainless D=12mm C=35mm
Rebar 1 D=12mm C=35mm
Rebar 2 D=12mm C=30mm
Stainless D=12mm C=30mm
Rebar 1 D=12mm C=15mm
Rebar 2 D=12mm C=10mm
Stainless D=12mm C=15mm

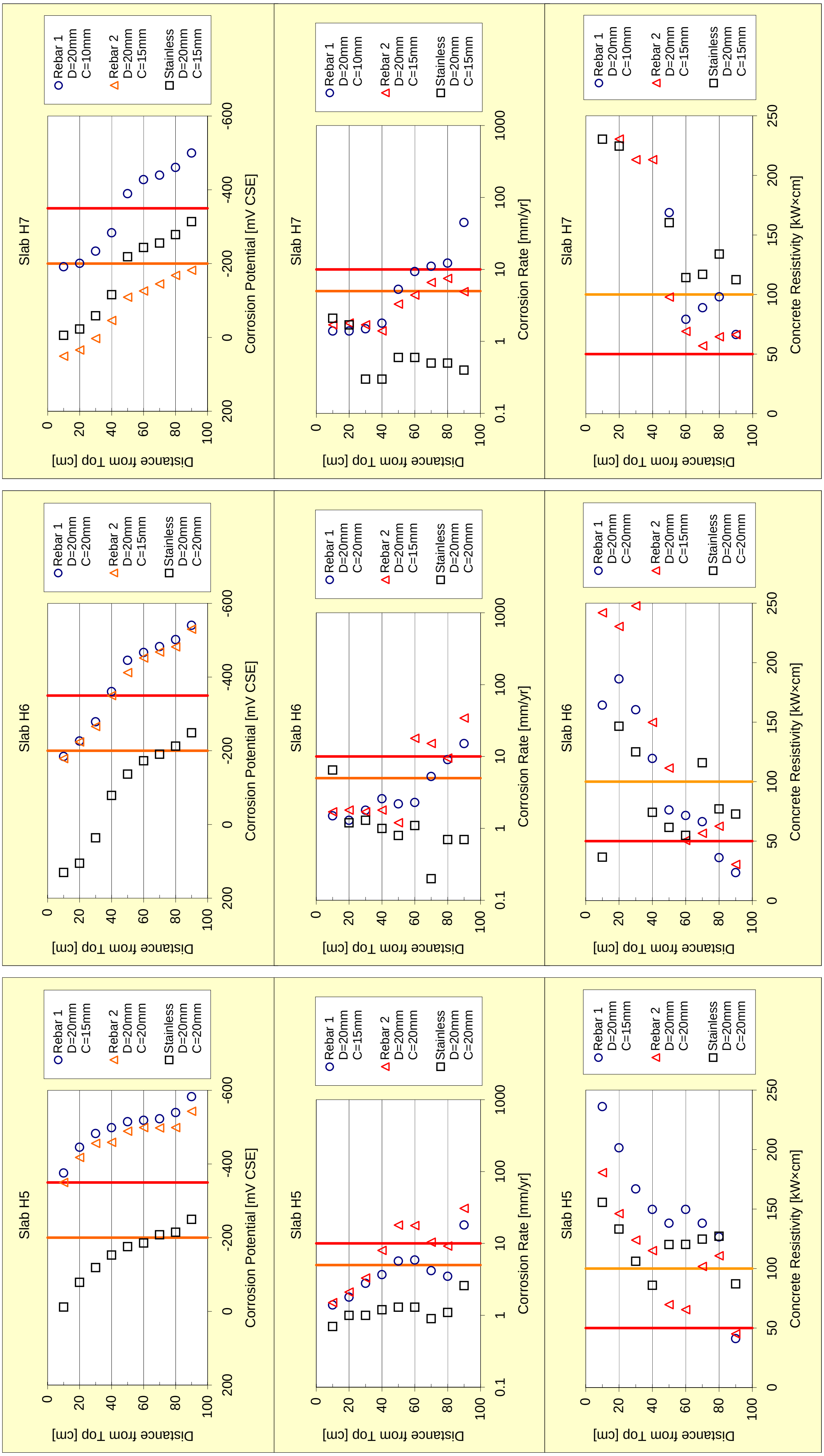
Slab H7
Slab H6
Slab H5
Distance from Top [cm]
Corrosion Potential [mV CSE]
Corrosion Rate [mm/yr]
Concrete Resistivity [kW×cm]
Rebar 1 D=20mm C=10mm
Rebar 2 D=20mm C=15mm
Stainless D=20mm C=15mm
Rebar 1 D=20mm C=20mm
Rebar 2 D=20mm C=15mm
Stainless D=20mm C=20mm
Rebar 1 D=20mm C=15mm
Rebar 2 D=20mm C=20mm
Stainless D=20mm C=20mm

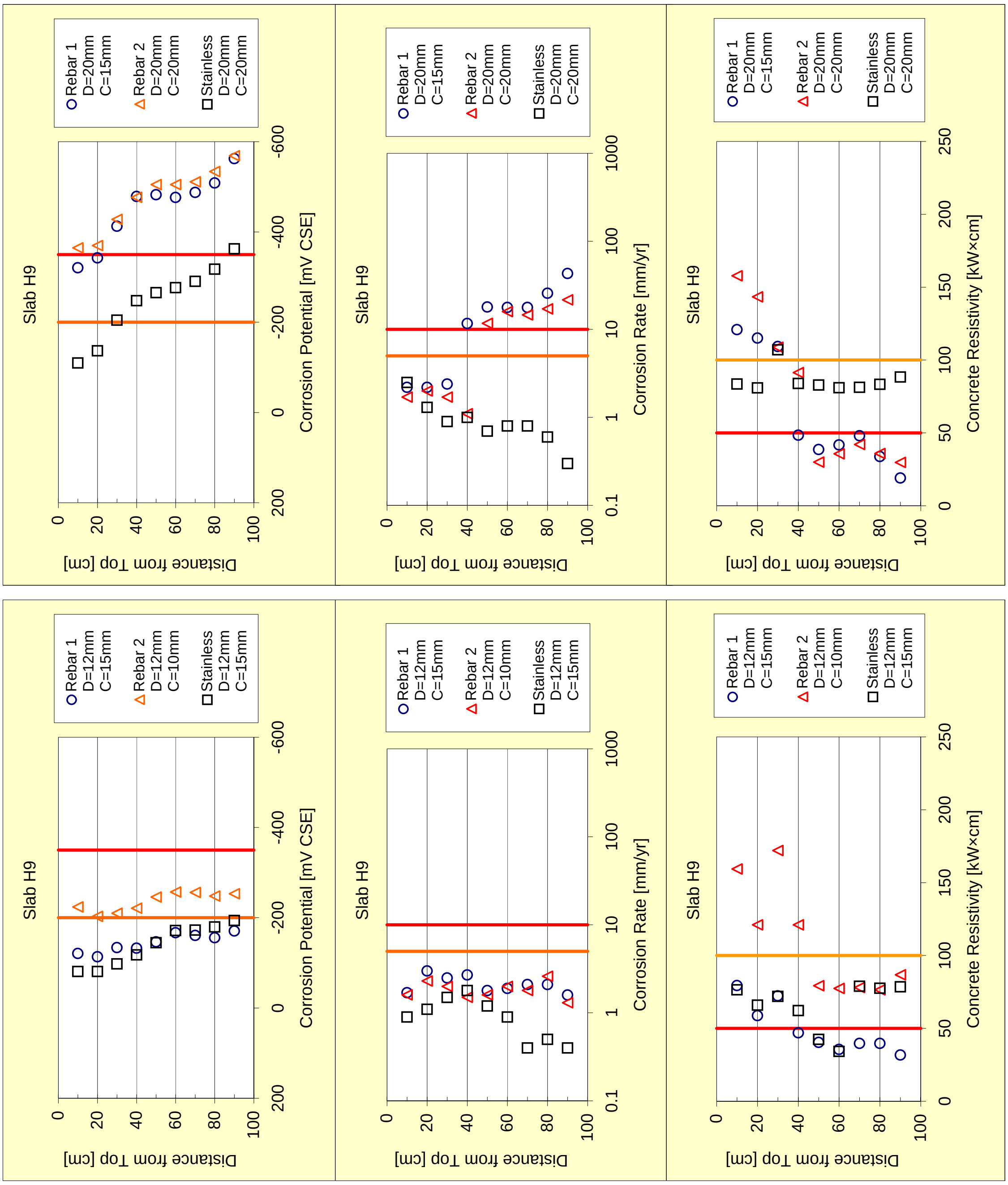
Slab H9
Distance from Top [cm]
Corrosion Potential [mV CSE]
Rebar 1 D=20mm C=15mm
Rebar 2 D=20mm C=20mm
Stainless D=20mm C=20mm
Slab H9
Distance from Top [cm]
Corrosion Rate [mm/yr]
Rebar 1 D=20mm C=15mm
Rebar 2 D=20mm C=20mm
Stainless D=20mm C=20mm
Slab H9
Distance from Top [cm]
Concrete Resistivity [kW×cm]
Rebar 1 D=20mm C=15mm
Rebar 2 D=20mm C=20mm
Stainless D=20mm C=20mm
Slab H9
Distance from Top [cm]
Corrosion Potential [mV CSE]
Rebar 1 D=12mm C=15mm
Rebar 2 D=12mm C=10mm
Stainless D=12mm C=15mm
Slab H9
Distance from Top [cm]
Corrosion Rate [mm/yr]
Rebar 1 D=12mm C=15mm
Rebar 2 D=12mm C=10mm
Stainless D=12mm C=15mm
Slab H9
Distance from Top [cm]
Concrete Resistivity [kW×cm]
Rebar 1 D=12mm C=15mm
Rebar 2 D=12mm C=10mm
Stainless D=12mm C=15mm

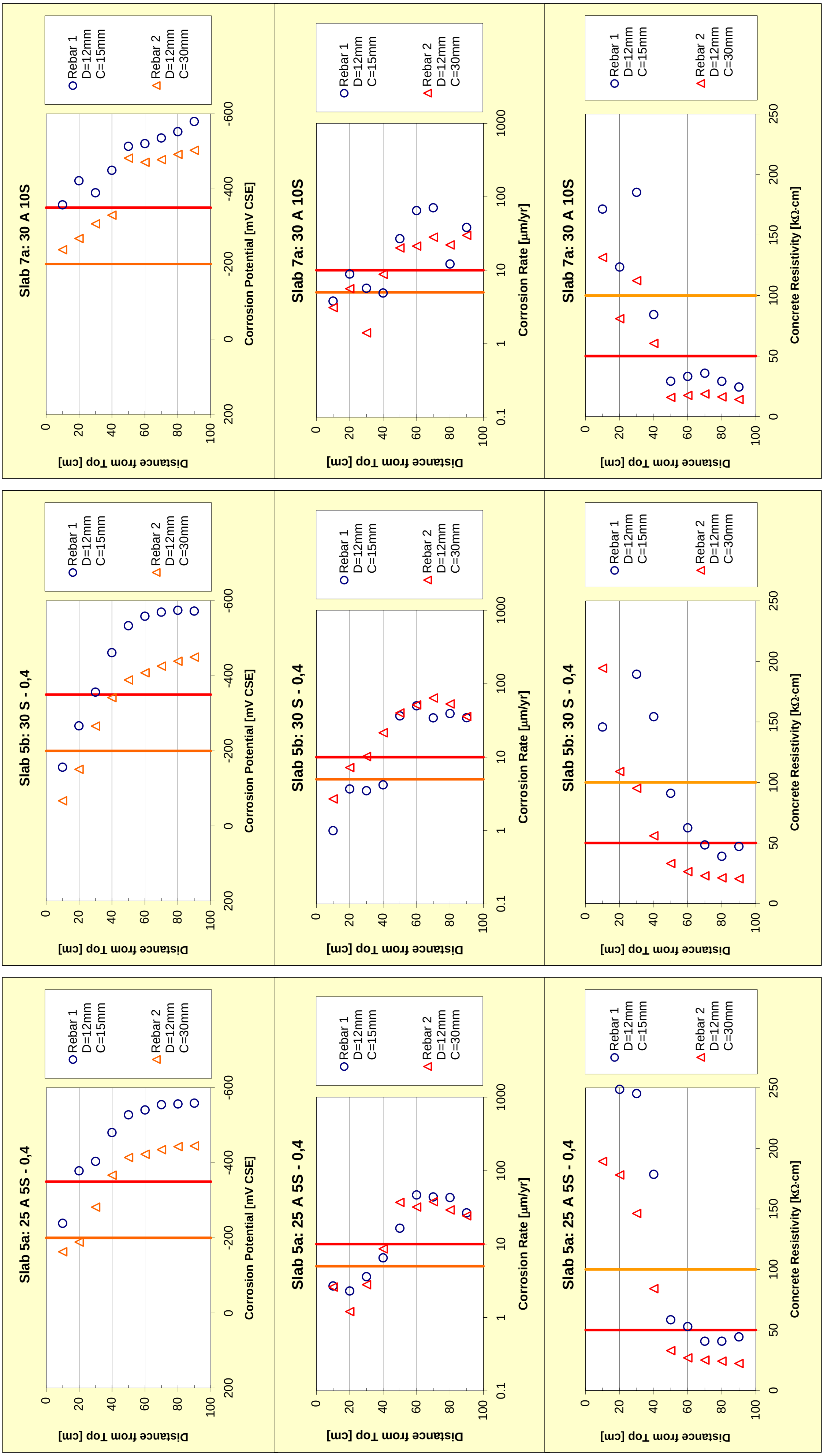
Slab 7a: 30 A 10S
Slab 5b: 30 S - 0,4
Slab 5a: 25 A 5S - 0,4
Rebar 1 D=12mm C=15mm
Rebar 2 D=12mm C=30mm
Distance from Top [cm]
Corrosion Potential [mV CSE]
Corrosion Rate [µm/yr]
Concrete Resistivity [kΩ·cm]

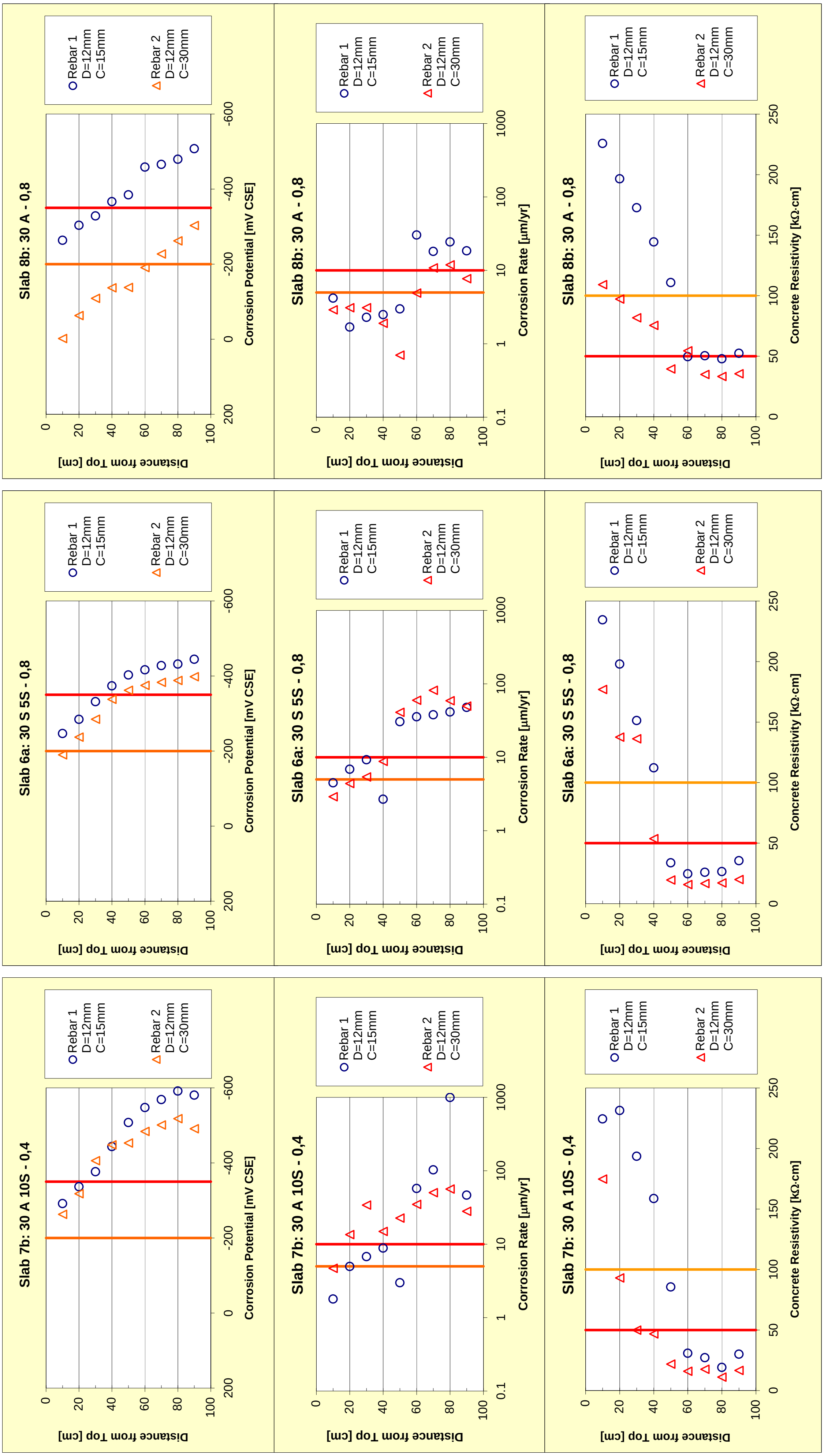
Slab 8b: 30 A - 0,8
Slab 6a: 30 S 5S - 0,8
Slab 7b: 30 A 10S - 0,4
Slab 7b: 30 A 10S - 0,4
Distance from Top [cm]
Corrosion Potential [mV CSE]
Corrosion Rate [µm/yr]
Concrete Resistivity [kΩ·cm]
Rebar 1 D=12mm C=15mm
Rebar 2 D=12mm C=30mm

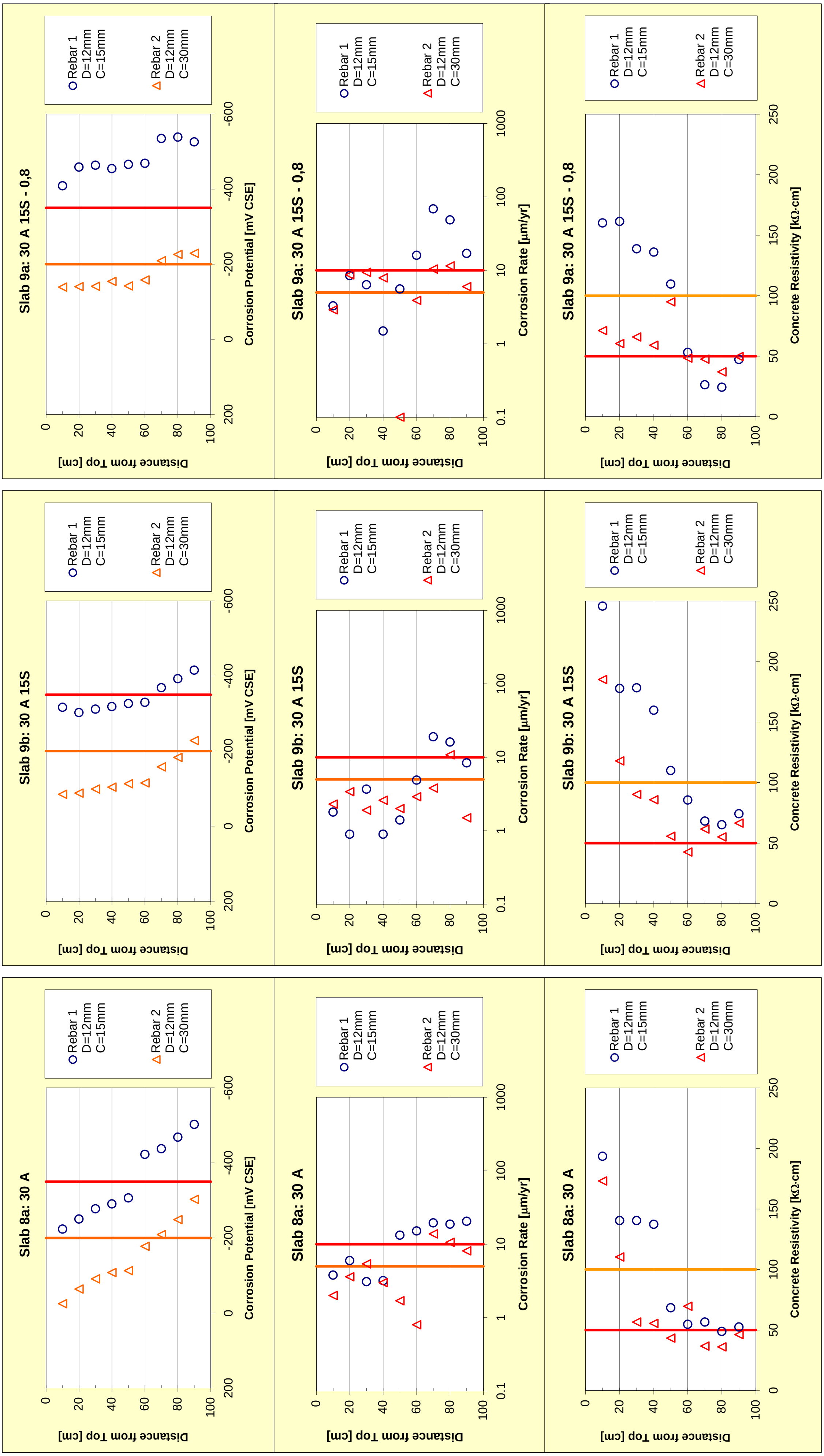
Slab 9a: 30 A 15S - 0,8
Slab 9b: 30 A 15S
Slab 8a: 30 A
Distance from Top [cm]
Corrosion Potential [mV CSE]
Corrosion Rate [µm/yr]
Concrete Resistivity [kΩ·cm]
Rebar 1 D=12mm C=15mm
Rebar 2 D=12mm C=30mm

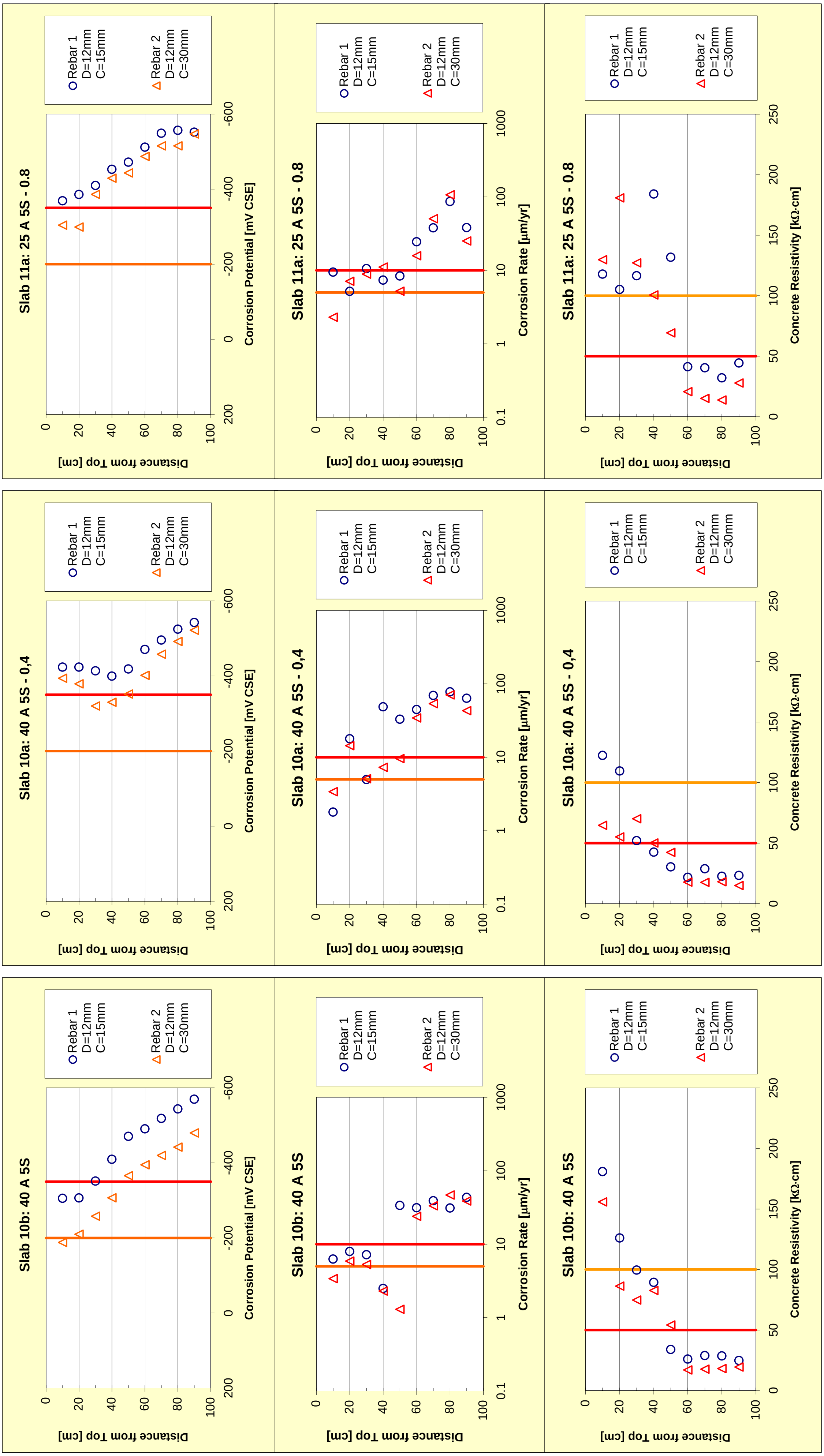
Slab 11a: 25 A 5S - 0.8
Slab 10a: 40 A 5S - 0,4
Slab 10b: 40 A 5S
Rebar 1 D=12mm C=15mm
Rebar 2 D=12mm C=30mm
Distance from Top [cm]
Corrosion Potential [mV CSE]
Corrosion Rate [µm/yr]
Concrete Resistivity [kΩ·cm]

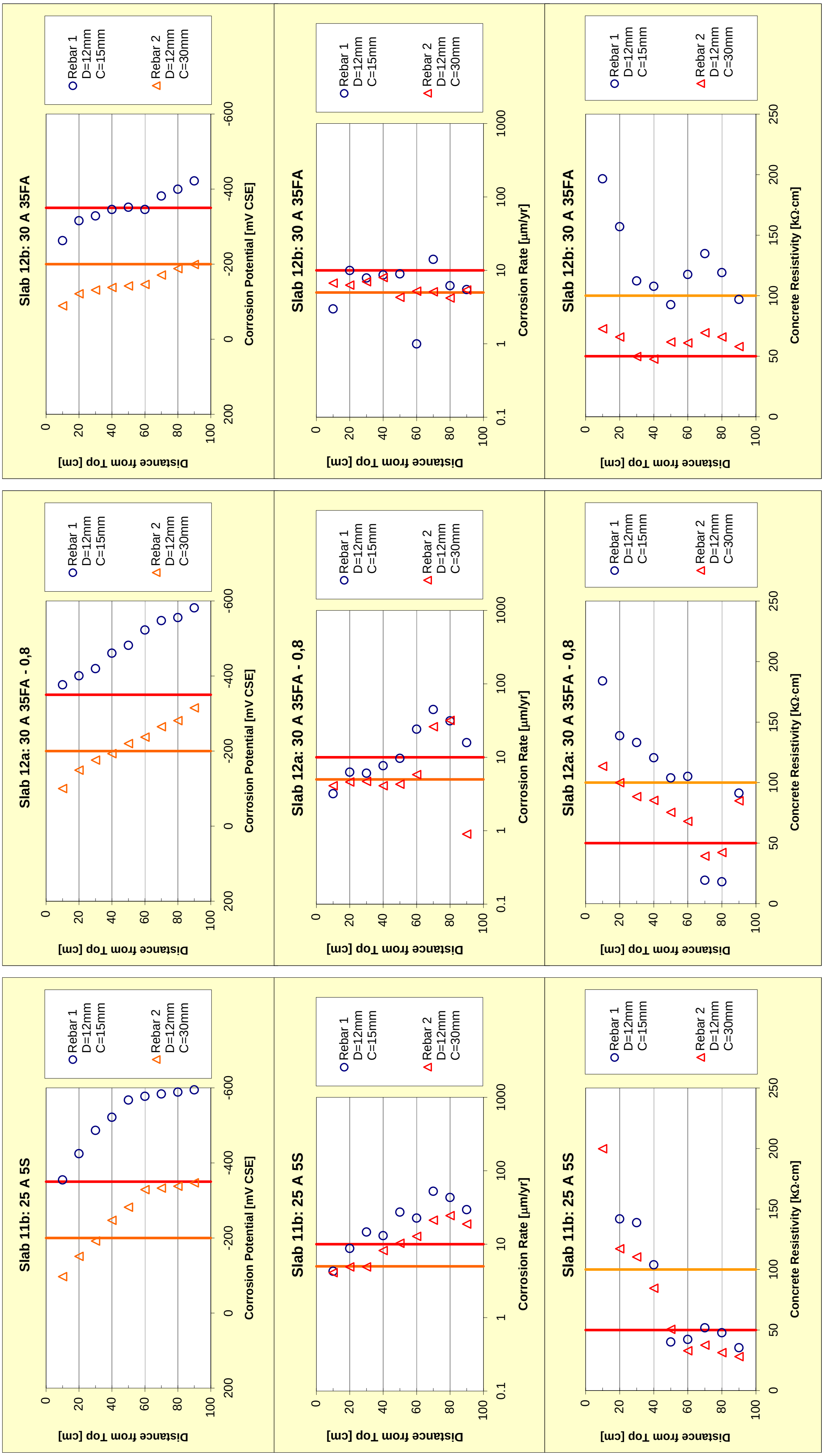
Slab 12b: 30 A 35FA
Slab 12a: 30 A 35FA - 0,8
Slab 11b: 25 A 5S
Distance from Top [cm]
Corrosion Potential [mV CSE]
Corrosion Rate [µm/yr]
Concrete Resistivity [kΩ·cm]
Rebar 1 D=12mm C=15mm
Rebar 2 D=12mm C=30mm
0
20
40
60
80
100
200
-200
-400
-600
0.1
1
10
1000
50
150
250

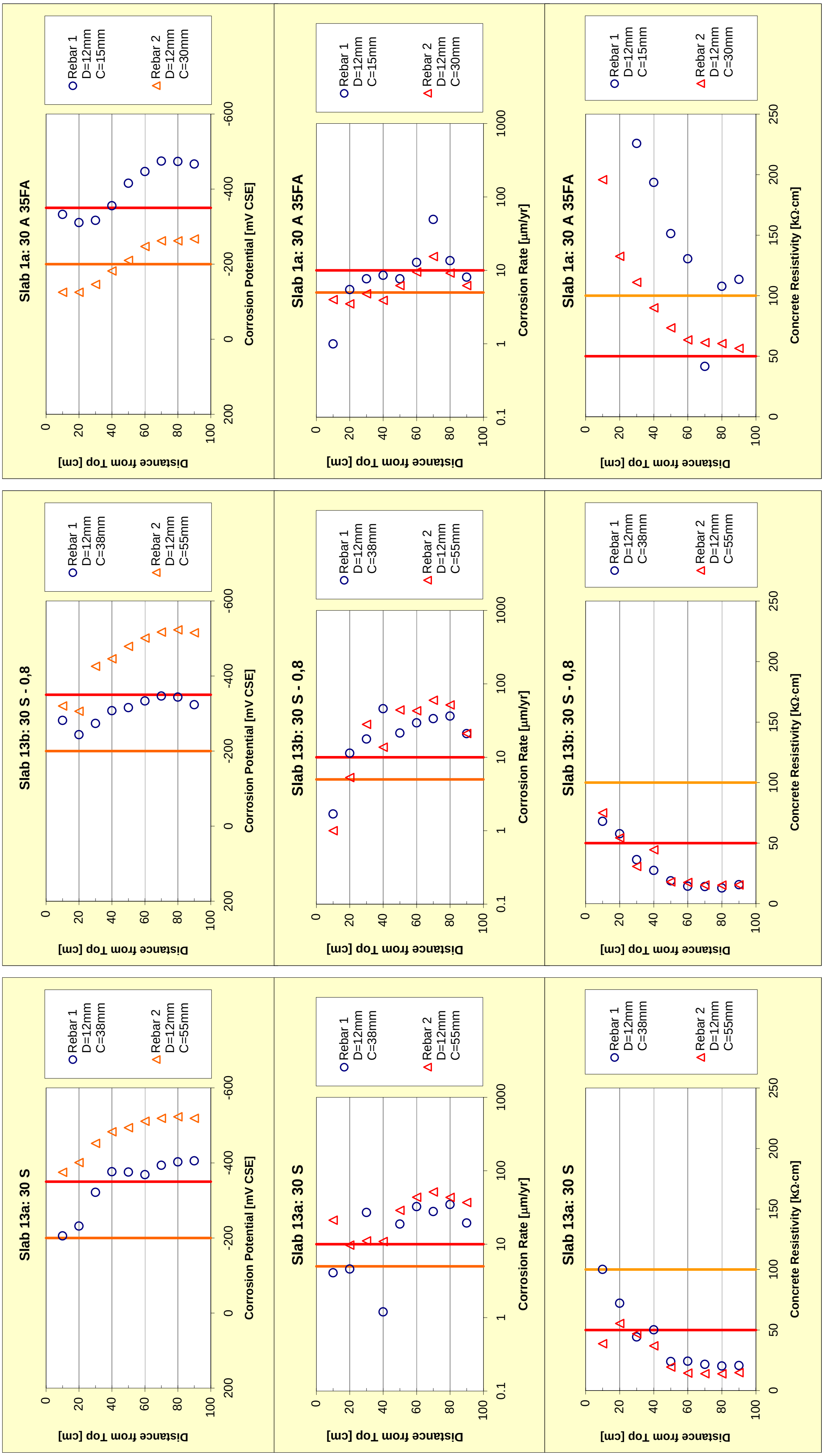
Slab 1a: 30 A 35FA
Slab 13b: 30 S - 0,8
Slab 13a: 30 S
Distance from Top [cm]
Corrosion Potential [mV CSE]
Corrosion Rate [µm/yr]
Concrete Resistivity [kΩ·cm]
Rebar 1 D=12mm C=15mm
Rebar 2 D=12mm C=30mm
Rebar 1 D=12mm C=38mm
Rebar 2 D=12mm C=55mm

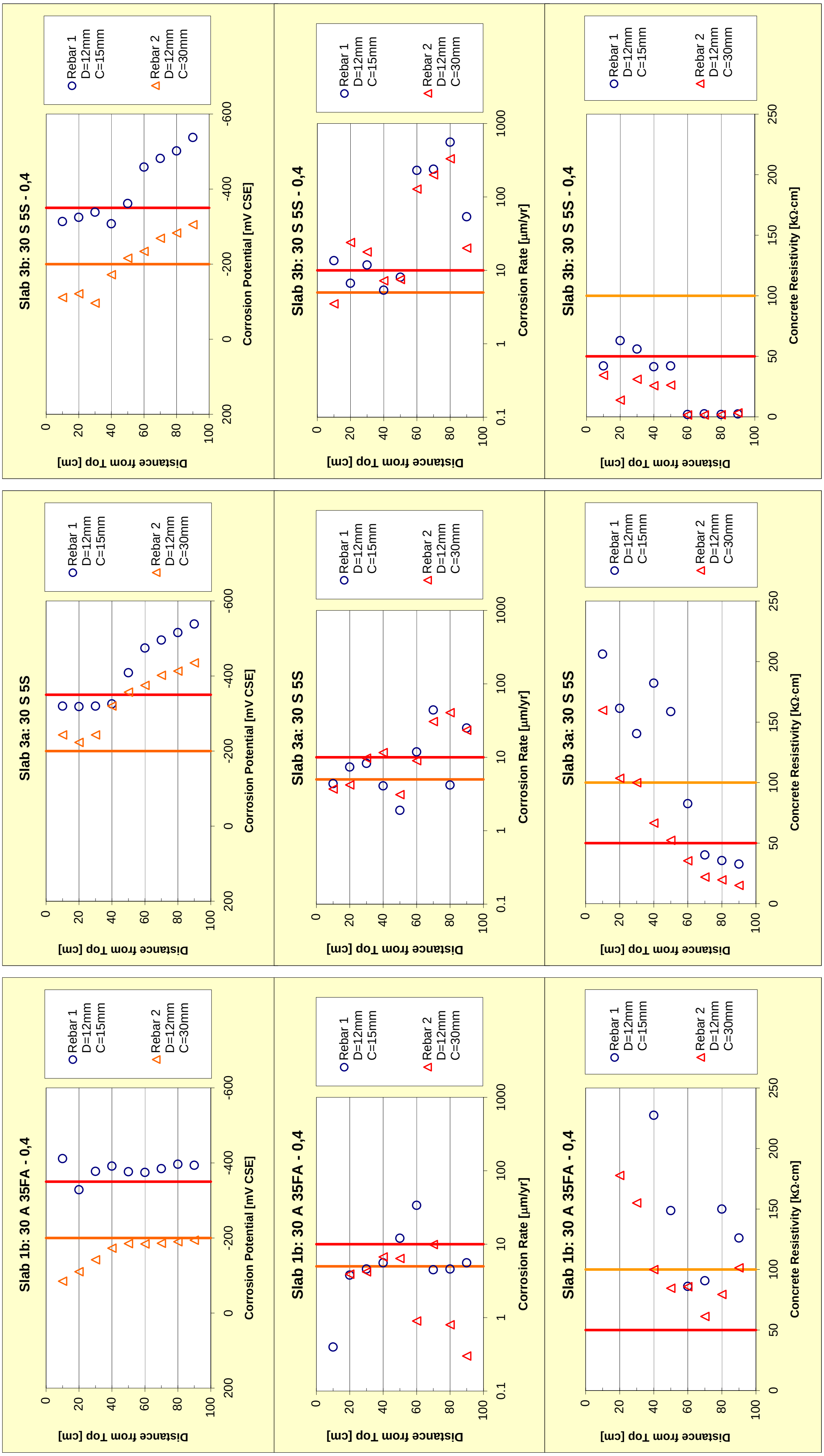
Slab 3b: 30 S 5S - 0,4
Distance from Top [cm]
Corrosion Potential [mV CSE]
Rebar 1 D=12mm C=15mm
Rebar 2 D=12mm C=30mm
Slab 3b: 30 S 5S - 0,4
Distance from Top [cm]
Corrosion Rate [µm/yr]
Rebar 1 D=12mm C=15mm
Rebar 2 D=12mm C=30mm
Slab 3b: 30 S 5S - 0,4
Distance from Top [cm]
Concrete Resistivity [kΩ·cm]
Rebar 1 D=12mm C=15mm
Rebar 2 D=12mm C=30mm
Slab 3a: 30 S 5S
Distance from Top [cm]
Corrosion Potential [mV CSE]
Rebar 1 D=12mm C=15mm
Rebar 2 D=12mm C=30mm
Slab 3a: 30 S 5S
Distance from Top [cm]
Corrosion Rate [µm/yr]
Rebar 1 D=12mm C=15mm
Rebar 2 D=12mm C=30mm
Slab 3a: 30 S 5S
Distance from Top [cm]
Concrete Resistivity [kΩ·cm]
Rebar 1 D=12mm C=15mm
Rebar 2 D=12mm C=30mm
Slab 1b: 30 A 35FA - 0,4
Distance from Top [cm]
Corrosion Potential [mV CSE]
Rebar 1 D=12mm C=15mm
Rebar 2 D=12mm C=30mm
Slab 1b: 30 A 35FA - 0,4
Distance from Top [cm]
Corrosion Rate [µm/yr]
Rebar 1 D=12mm C=15mm
Rebar 2 D=12mm C=30mm
Slab 1b: 30 A 35FA - 0,4
Distance from Top [cm]
Concrete Resistivity [kΩ·cm]
Rebar 1 D=12mm C=15mm
Rebar 2 D=12mm C=30mm

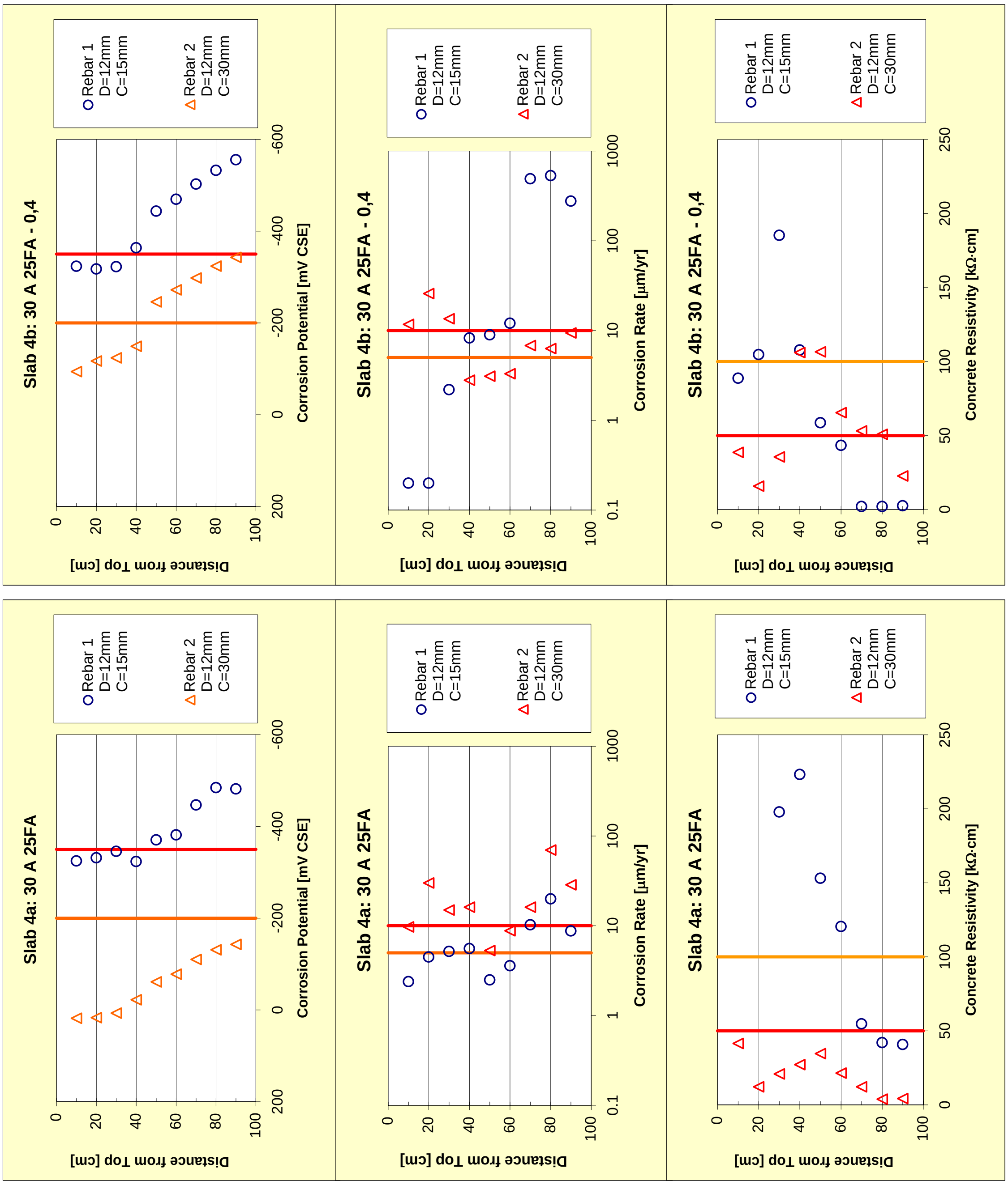

Slab 4b: 30 A 25FA - 0,4
Slab 4a: 30 A 25FA
Rebar 1 D=12mm C=15mm
Rebar 2 D=12mm C=30mm
Distance from Top [cm]
Corrosion Potential [mV CSE]
Corrosion Rate [µm/yr]
Concrete Resistivity [kΩ·cm]

Rebars in Slab 1-352 (100% PC, w/b 0.35)

Rebar 1

Rebar 2

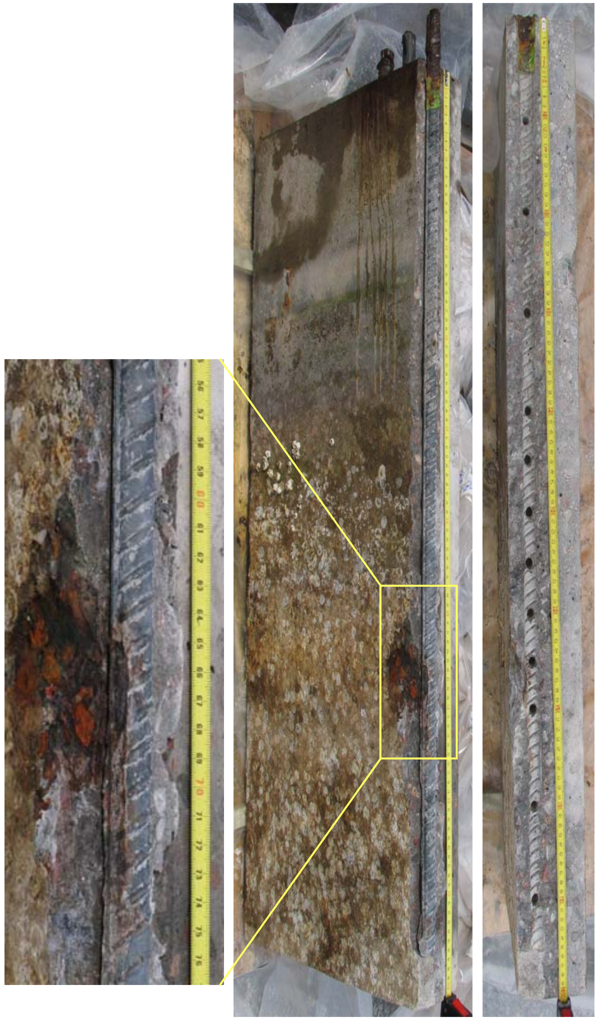

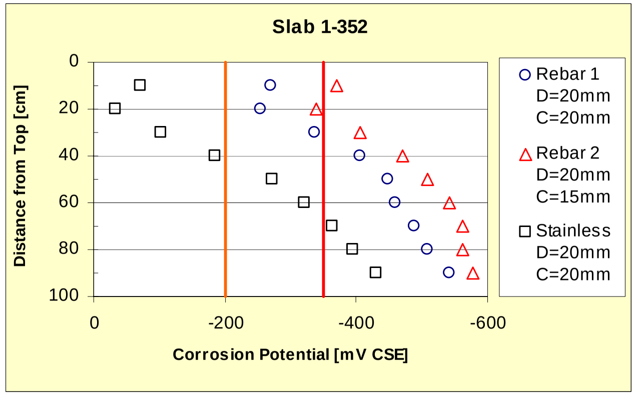

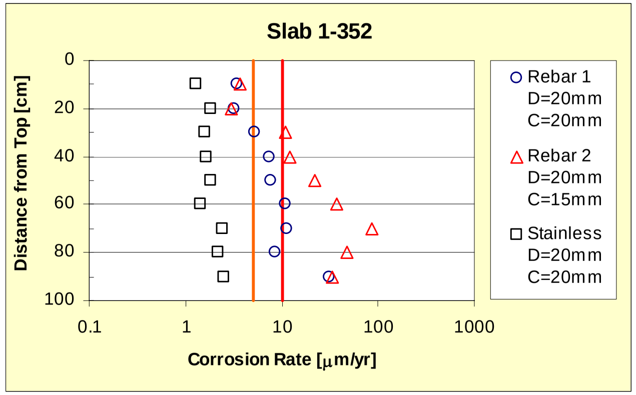

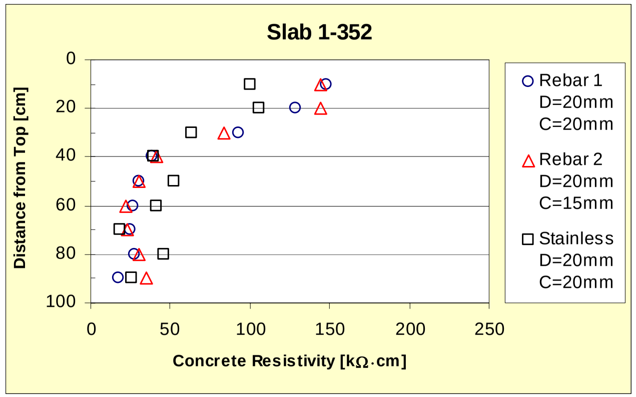

Rebars in Slab 7-40 (100% PC, w/b 0.40)

Rebar 1

Rebar 2

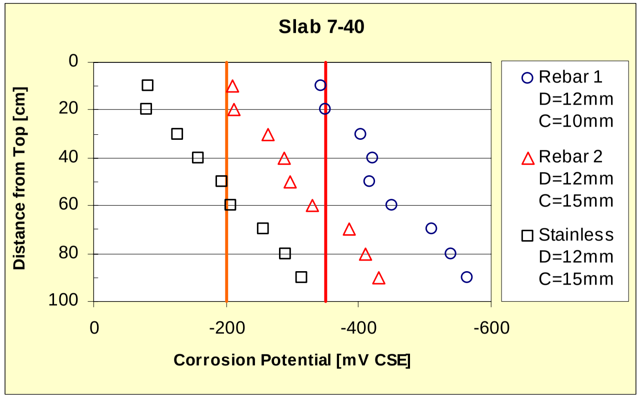

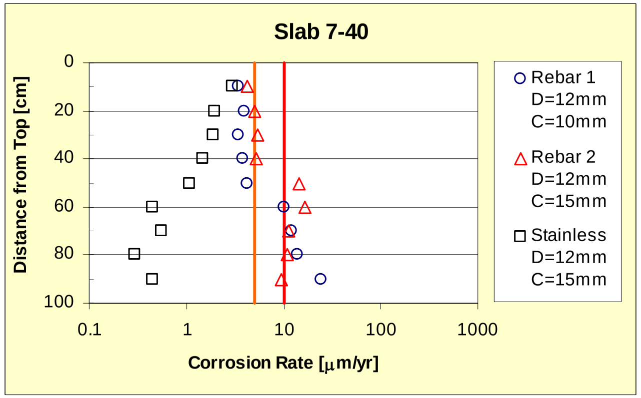

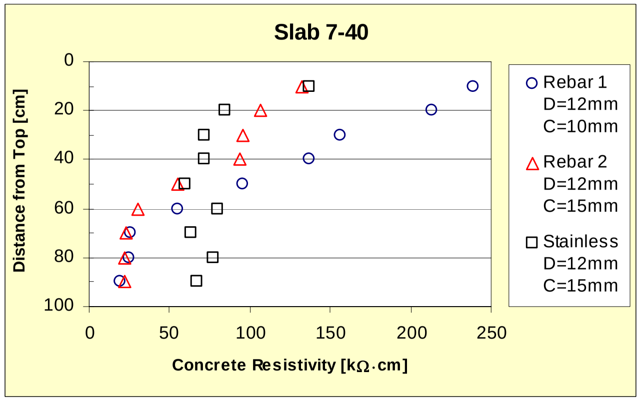

Rebars in Slab 4-40 (90% PC+10%SF, w/b 0.40)

Rebar 1

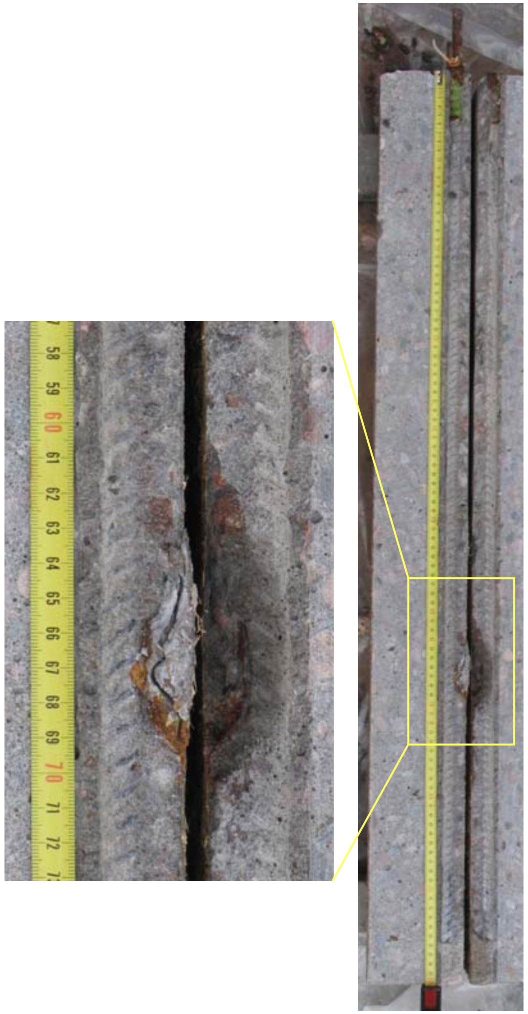

Rebar 2

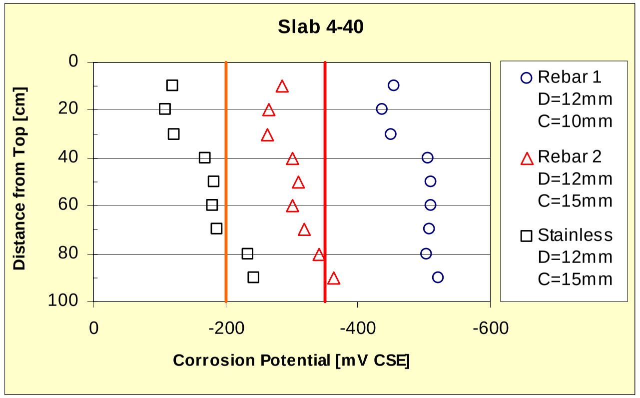

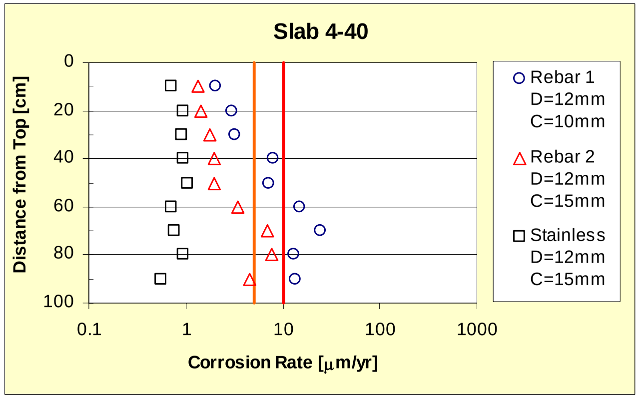

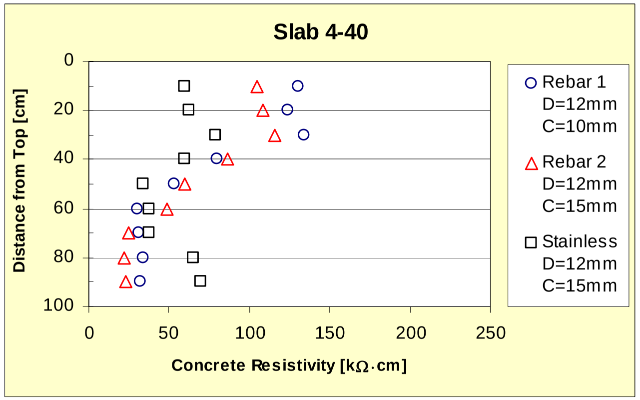

Rebars in Slab 10-40 (78.5%PC+17%FA+4.5%SF, w/b 0.40)

Rebar 1

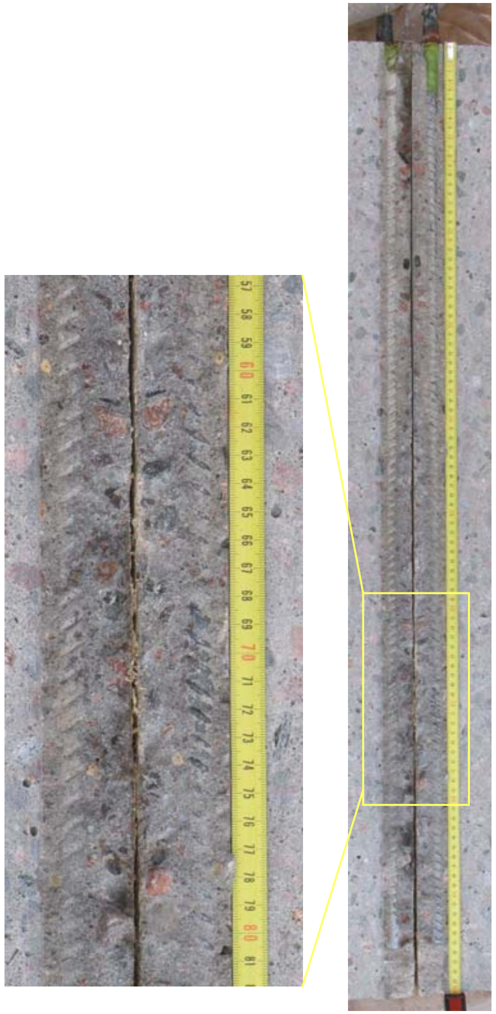

Rebar 2

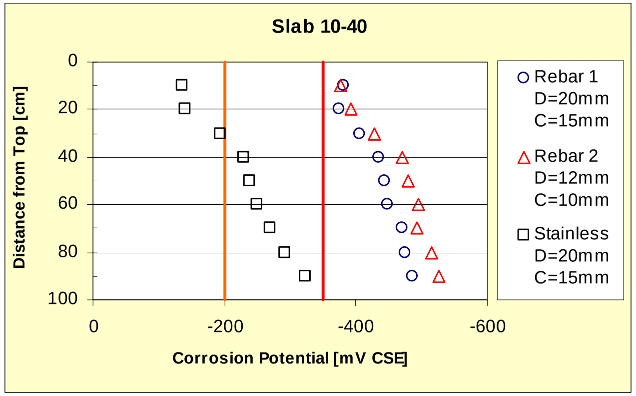

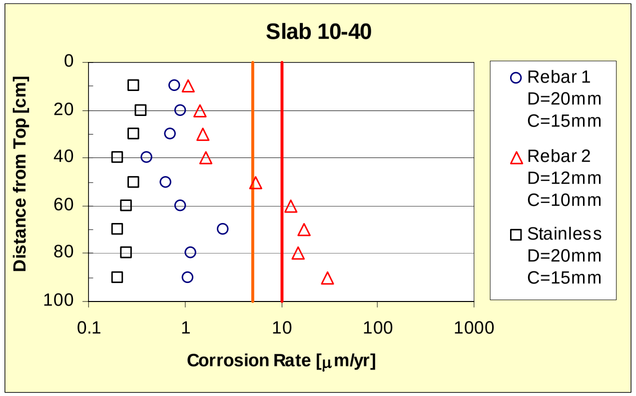

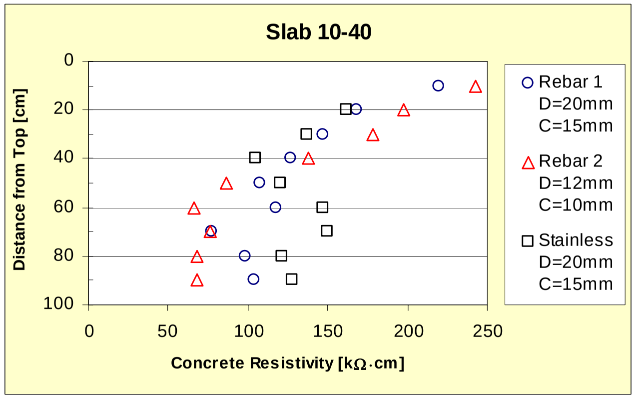

Rebars in Slab H8 (80%PC+20%FA, w/b 0.30)

Rebar 1

Rebar 2

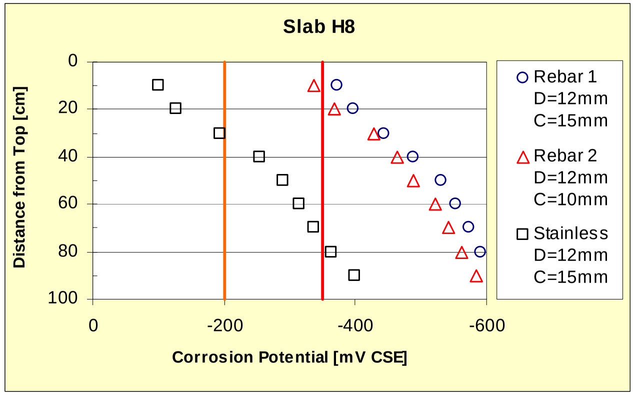

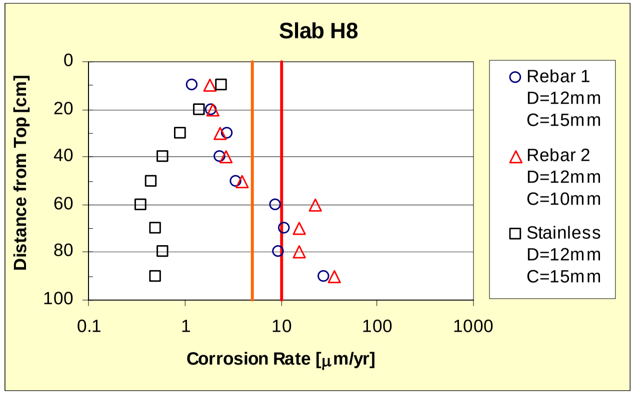

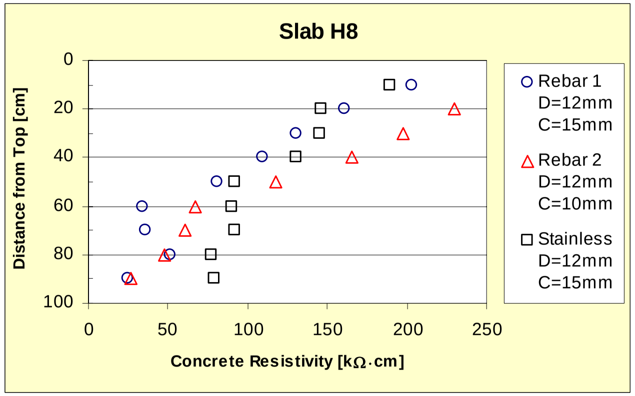

Rebars in Slab 1a (35% FA, w/b 0.30)

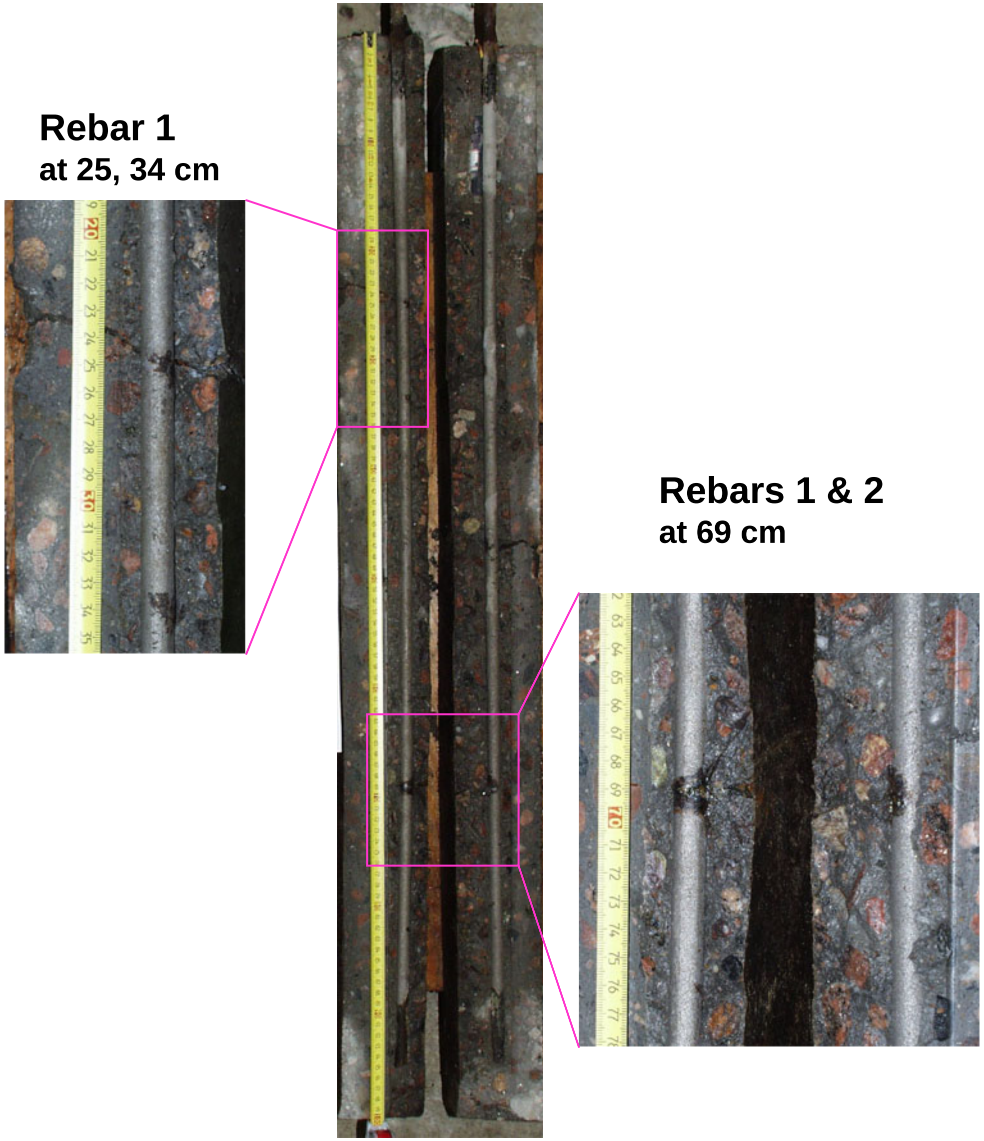

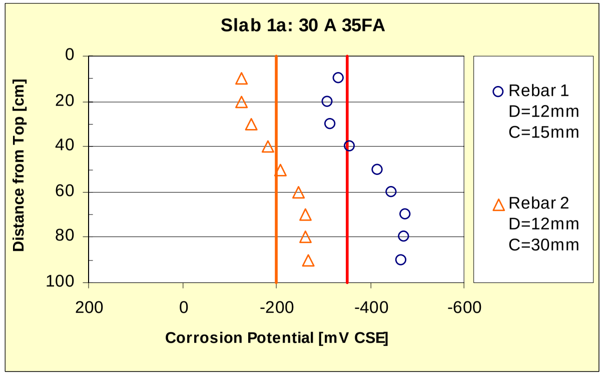

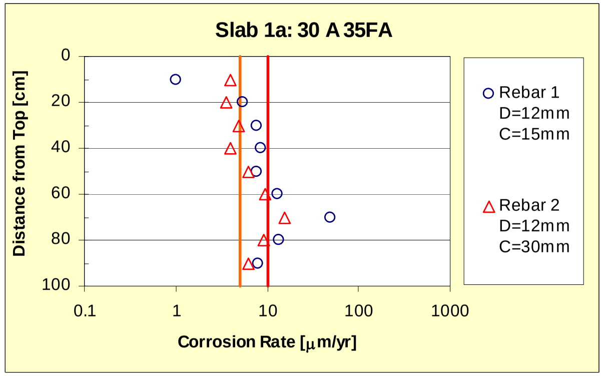

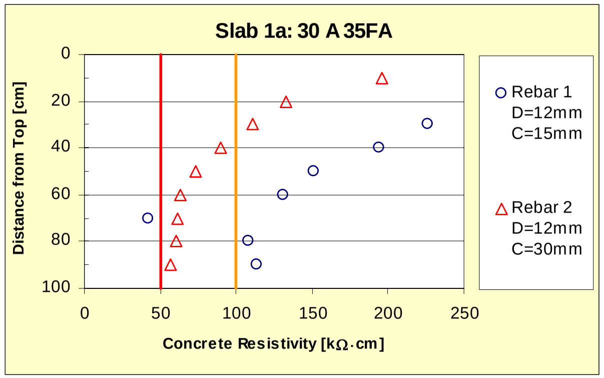

Rebars in Slab 7a (90% PC+10%SF, w/b 0.30)

Rebars 2 & 1
Corrosion at 21, 29 cm

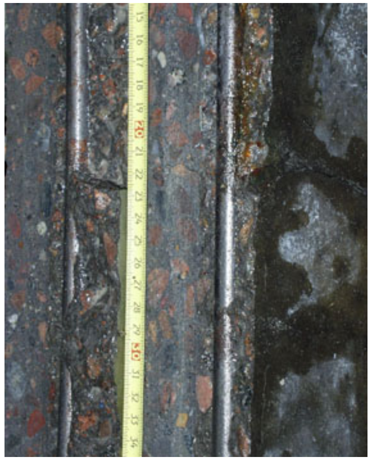

Rebars 2 & 1
Corrosion at 90-95 cm

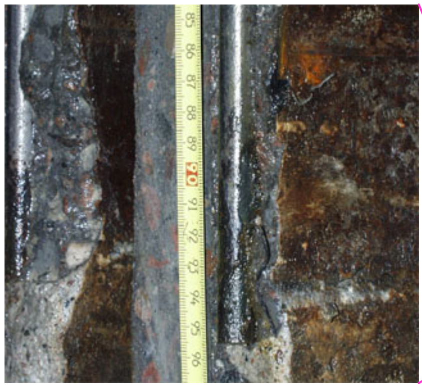

Rebar 1
Corrosion at 66, 78 cm

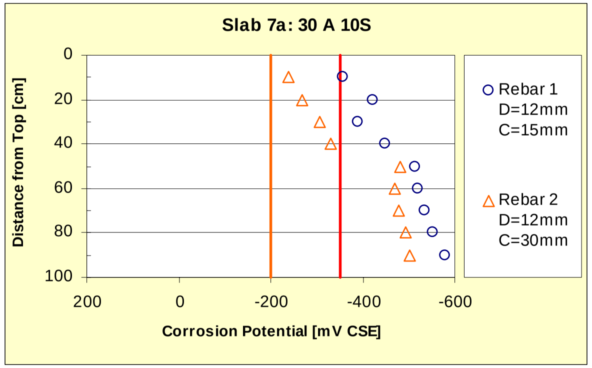

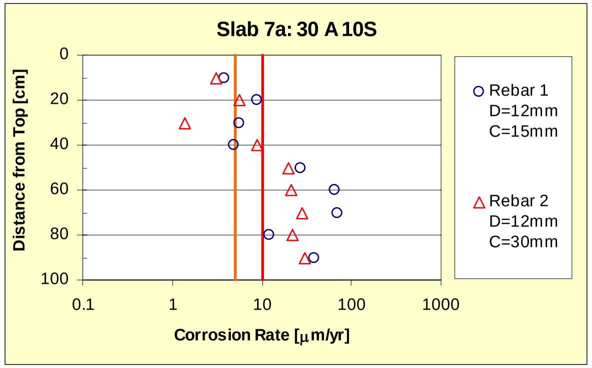

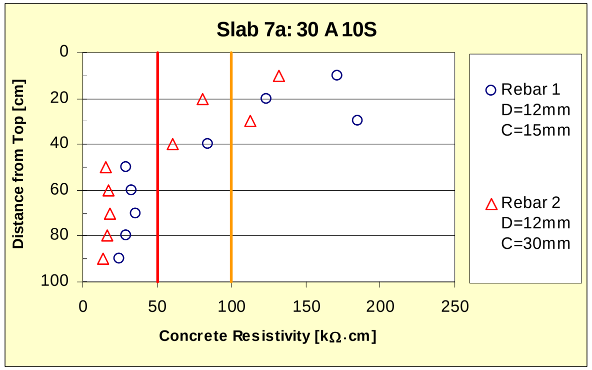

Rebars in Slab 8a (100% PC, w/b 0.30)

Rebar 1
Corrosion at 24, 33 cm

Rebar 1
Corrosion at 75-80 cm

Rebar 2
Corrosion at 73 cm

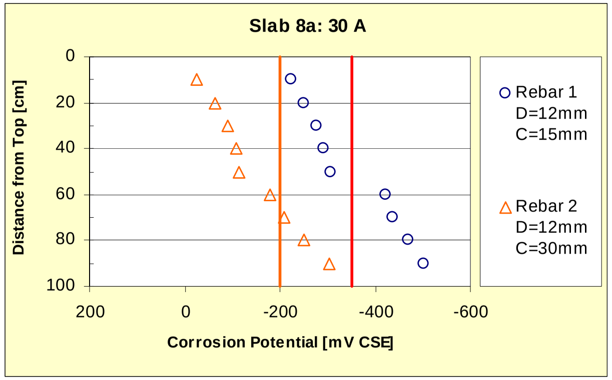

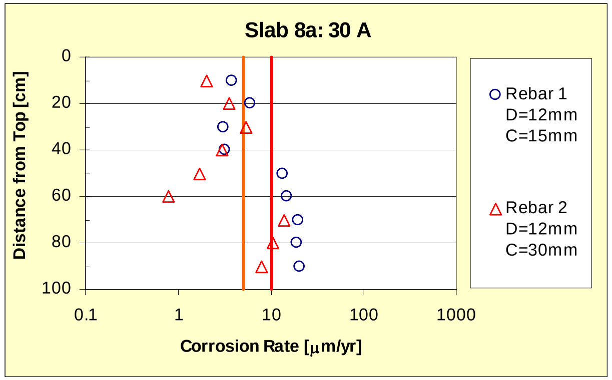

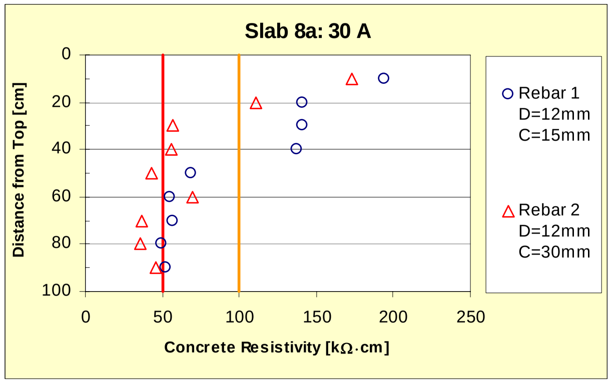

Rebars in Slab 10-40 (78.5%PC+17%FA+4.5%SF, w/b 0.40)

Rebars 2 & 1
Corrosion at 21 cm

Rebar 1
Corrosion at 53 cm

Rebars 2 & 1
Corrosion at 61, 74 cm